Coacervate Droplets for Synthetic Cells

Zi Lin, Thomas Beneyton, Jean-christophe Baret, Nicolas Martin

small methods
www.small-methods.com

Coacervate Droplets for Synthetic Cells

*Zi Lin, Thomas Beneyton, Jean-Christophe Baret, and Nicolas Martin**

The design and construction of synthetic cells – human-made microcompartments that mimic features of living cells – have experienced a real boom in the past decade. While many efforts have been geared toward assembling membrane-bounded compartments, coacervate droplets produced by liquid–liquid phase separation have emerged as an alternative membrane-free compartmentalization paradigm. Here, the dual role of coacervate droplets in synthetic cell research is discussed: encapsulated within membrane-enclosed compartments, coacervates act as surrogates of membraneless organelles ubiquitously found in living cells; alternatively, they can be viewed as crowded cytosol-like chassis for constructing integrated synthetic cells. After introducing key concepts of coacervation and illustrating the chemical diversity of coacervate systems, their physicochemical properties and resulting bioinspired functions are emphasized. Moving from suspensions of free floating coacervates, the two nascent roles of these droplets in synthetic cell research are highlighted: organelle-like modules and cytosol-like templates. Building the discussion on recent studies from the literature, the potential of coacervate droplets to assemble integrated synthetic cells capable of multiple life-inspired functions is showcased. Future challenges that are still to be tackled in the field are finally discussed.

1. Introduction

Living cells are fascinating self-sustained compartmentalized chemical systems able to sense and adapt to their environment, self-repair, grow, divide, and evolve. Albeit indisputably challenging, reproducing such complex behaviors in human-made soft microcompartments has emerged as a new field of research in its own. Synthetic cells can be defined as artificial microcompartments that recapitulate essential functions of living cells, regardless of the molecular components they are assembled from. The construction of synthetic cells constitutes a benchmark of our understanding of living systems. The bottom-up reconstitution of biological functions using a minimal set of well-defined modules is indeed an extremely powerful approach to tackle yet unanswered questions in extant biology by dissecting complex cellular processes. Beyond biological parts, the construction of synthetic cells also takes advantage of rationally designed synthetic components. This chemical diversity provides new avenues to shed light on the transition from inanimate to living matter by exploring how self-organization may emerge in synthetic compartments. A reengineering approach making use of both biological entities and artificial or synthetic parts therefore provides a methodology to explore this transition as a universal problem, and at the same time sets the ground for future applications.

Inspired by the membranous structure of living cells, many efforts have been devoted to the fabrication of synthetic cells in the form of membrane-bounded microcompartments able to capture essential cellular functions, such as selective permeability or catalysis. Yet, cells are highly crowded environments where thousands of biomolecules dynamically interact and react together. Integrating such a molecularly dense milieu in the design of synthetic cells is therefore becoming crucial. In this vibrant research area, a long-known phenomenon has recently been brought back to light: liquid–liquid phase separation.

Associative liquid–liquid phase separation (LLPS) in aqueous polymer solutions produces polymer-rich microdroplets known as "coacervates." This phenomenon was first serendipitously observed by German scientist Tieback more than a century ago in mixtures of charged proteins and polysaccharides,[1] but only later coined "coacervation" (from the Latin "acervare" meaning "to pile up" or "to heap") and systematically studied by Dutch chemists Bungenberg de Jong and Kruyt.[2] The biological importance of coacervates has been intuited ever since: in their pioneering works, Bungenberg de Jong and Kruyt already pointed to the analogy between coacervates and the crowded intracellular milieu,[2] while a few years later, Russian chemist Oparin hypothesized that coacervates could have played a role as primitive forms of cells ("protocells") in the origins of life due to their ability to concentrate chemically reactive species.[3]

These early intuitions were mostly overlooked in the following years, while in the meantime, many applications of coacervates emerged in fields as varied as cosmetics,[4] food science,[5] or underwater adhesion,[6] and theories on coacervation were

Z. Lin, T. Beneyton, J.-C. Baret, N. Martin
Université de Bordeaux
CNRS
Centre de Recherche Paul Pascal
UMR5031, 115 avenue du Dr. Schweitzer, 33600 Pessac, France
E-mail: nicolas.martin@crpp.cnrs.fr

The ORCID identification number(s) for the author(s) of this article can be found under https://doi.org/10.1002/smtd.202300496

DOI: 10.1002/smtd.202300496

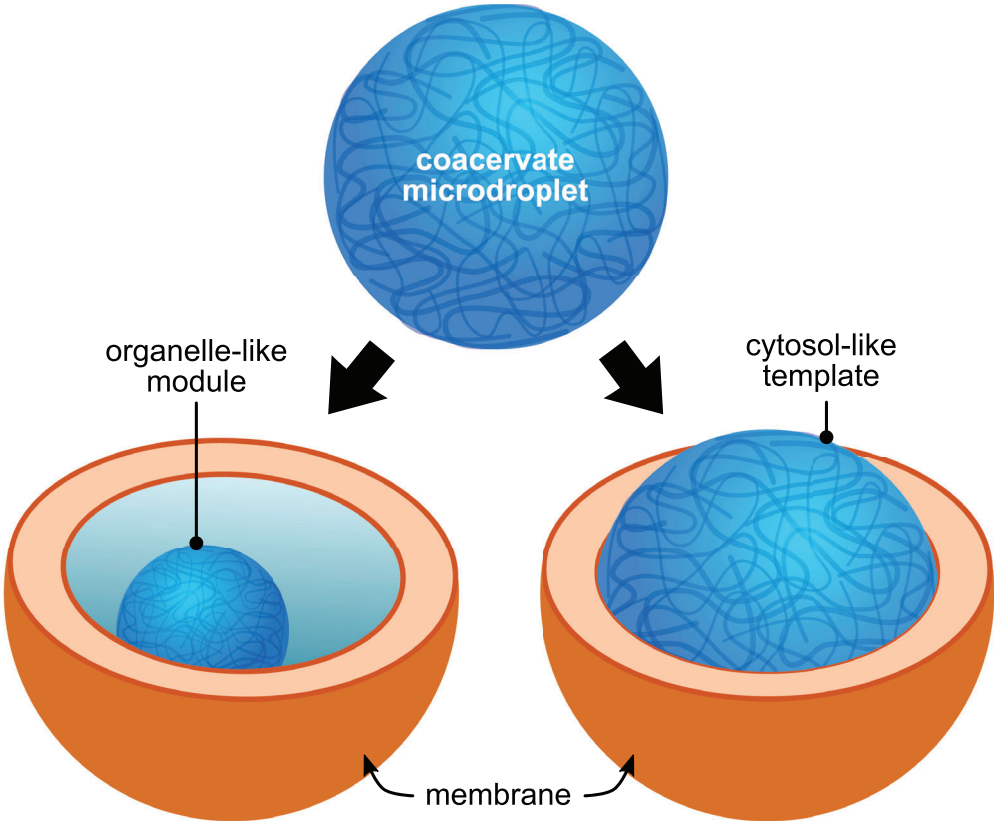

Figure 1. Schematic illustration of the dual role of coacervate droplets in synthetic cells research. Encapsulated within membrane-bounded compartments, coacervates play the role of organelle-like modules. Alternatively, coacervates can serve as cytosol-like templates for the construction of integrated synthetic cells.

developed.[7,8] Recent discoveries are now refueling the parallel between coacervates, biological systems, and protocells.[9] On the one hand, the past decade has witnessed the discovery of a new class of intracellular organelles that lack a lipid membrane,[10] as opposed to the canonical membrane-bounded organelles found in eukaryotic cells (such as the nucleus, mitochondria, or the Golgi apparatus). These membraneless organelles, also called biomolecular condensates, form in cellulo by an associative LLPS process involving proteins and polynucleotides[11] and share many properties with coacervate droplets.[12,13] On the other hand, reports revealing that coacervates could assemble from low molecular weight species rather than polymers[14–16] (including biologically or prebiotically relevant molecules such as mononucleotides and oligopeptides) and could host catalytic reactions[17] have reignited interest in the role of these droplets as protocells.[18,19] The design of organelle-inspired or protocell-like coacervates is now fueling the construction of more complex ensembles.

After introducing some basics of coacervation, we classify the key bioinspired properties of coacervate droplets that make them relevant tools to build synthetic cells. Moving from suspensions of free floating coacervates, we then illustrate the two nascent directions that are emerging: coacervates as organelles-like modules within membrane-bounded compartments or as cytosol-like templates for the assembly of integrated synthetic cells (**Figure 1**).

2. Basics of Coacervation

2.1. Segregative versus Associative Liquid–Liquid Phase Separation

LLPS is a thermodynamically driven phenomenon that describes the demixing of aqueous solutions of polymers, proteins, molecular amphiphiles, salts, or other solutes into two immiscible aqueous phases with different solute concentrations at equilibrium. LLPS is evidenced in macroscopic bulk systems by the formation of a turbid suspension of micrometer-sized droplets under appropriate conditions (concentration, temperature, pH, ionic strength, etc.). These droplets coarsen over time, ultimately resulting in the macroscopic separation of the two phases. LLPS is subdivided into two main classes: segregative or associative LLPS (**Figure 2**).

Segregative LLPS typically involves two (or more) polymers in water that form two coexisting phases at equilibrium, each enriched in one or the other species, and conventionally referred to as aqueous two-phase systems.[20] The seminal example of segregative LLPS is the phase separation of poly(ethylene glycol) (PEG) and dextran – a natural polysaccharide – into two aqueous phases enriched in either one or the other polymer. Segregative LLPS has generally been associated to polymer incompatibility, although a net repulsion between polymers is not always

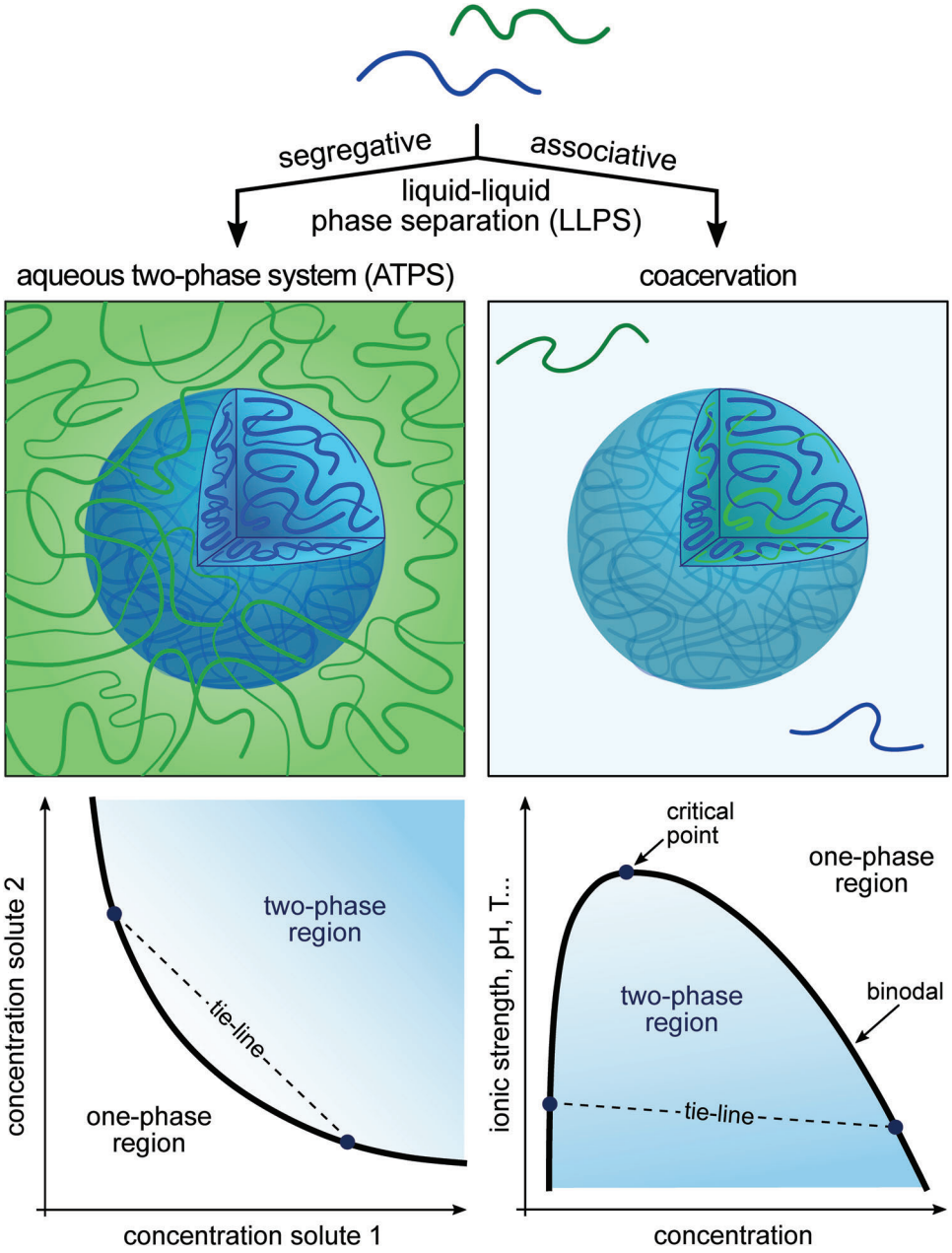

Figure 2. Schematic view of segregative versus associative liquid–liquid phase separation, and associated illustrative phase diagrams.

needed since polymer–solvent interactions may also drive phase separation.[21]

Associative LLPS, better known as "coacervation" produces a phase enriched in solutes (the coacervate phase) in equilibrium with a solute-depleted phase (the supernatant phase). Polymer-based coacervation is a long-known phenomenon that has been categorized as "simple coacervation" when it involves a single species and "complex coacervation" when it relies on the pairing of oppositely charged polyions. Typical phase diagrams of coacervation show two regions that identify conditions for which phase separation occurs and that are separated by the binodal curve (Figure 2). Within the phase-separated region, tie lines connect the two points corresponding to the coacervate and associated supernatant phases, respectively. Limiting conditions at which phase separation no longer occurs define a critical point on the binodal.

The classical Flory–Huggins lattice theory of polymer mixing[22] (combined to the Debye–Huckel theory of simple electrolytes for complex coacervation[7,8]) provides a simple analytical form for the free energy of polymer-based segregative and associative LLPS that predicts well general trends of phase separation. Accessing a more detailed theory of polyelectrolyte complex coacervation is yet not trivial due to strong Coulombic interactions, charge connectivity on polymer chains, and the different length scales involved, and is therefore still an active area of research.[23–25]

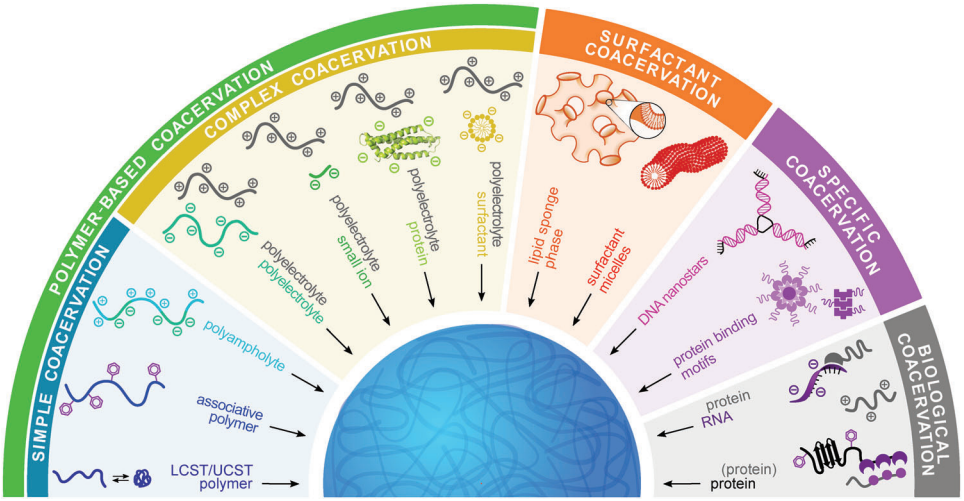

Figure 3. Schematic representation of the chemical diversity of coacervate systems used in synthetic cell research. Polymer and surfactant coacervation is driven by nonspecific, multivalent interactions. Specific nucleotide pairing interactions or protein binding motifs can also drive phase separation. Biological coacervates refer to more complex ensembles that may involve an intricate combination of both nonspecific and specific interactions.

In this review, we focus on the use of associative LLPS in synthetic cell research, although pioneering works have also demonstrated the significance of segregative LLPS for the construction of cell-mimetic compartments.[26,27]

2.2. The Coacervate Toolbox: Chemical Diversity and Driving Forces of Coacervation

Polyelectrolyte-based complexes have historically been the ground for bioinspired coacervates. Yet, a great variety of coacervates has been formulated and characterized since the first discovery of complex coacervates in the early XXth century (**Figure 3**). In recent years, "coacervation" has thus been used as a generic term to describe the formation of liquid-like, chemically rich microdroplets suspended in a dilute continuous aqueous phase. Although these systems are not all biologically relevant, they give access to a rich palette of phase separating systems for the design of synthetic cells. A common feature of all these systems is that they form via noncovalent multivalent interactions between their constitutive molecules. In most cases, these interactions are nonspecific (e.g., electrostatic interactions, H-bonding, π–π stacking...), but coacervate-like droplets that rely on specific interactions have also emerged recently. We here briefly exemplify the chemical diversity of coacervate-like systems and discuss the driving forces of phase separation depending on the chemical nature and interactions between phase-separating species.

2.2.1. Polymer-Based Coacervation

Simple Coacervation: Simple coacervation, also known as self-coacervation, refers to the phase separation of a single polymer specie. It is typically observed under desolvating conditions, whereby polymers experience a change from good to poor solvent either due to an added chemical (such as salt or a water-miscible organic solvent) or upon a change in temperature (for upper- and lower-critical-solution-temperature (UCST and LCST)-type polymers). Well-known examples of biologically relevant LCST-type polymers that form liquid-like coacervates upon heating are elastin-like polypeptides (ELPs) in which repeating amino acid pentamer sequence can be engineered to tune the transition temperature.[28,29] Notably, such a LCST behavior has also recently been demonstrated for purine-containing single-stranded DNA (ssDNA) in the presence of magnesium cations, allowing the formation of all-DNA simple coacervates.[30–32]

Associative polymers and polyampholytes are also prone to undergo simple coacervation. Polyampholytes are polymers that bear both positive and negative charges and undergo self-coacervation via a process akin to complex coacervation (see below).[33,34] In comparison, associative polymers contain strongly interacting moieties (also called "sticky" motifs, such as hydrophobic side chains) that bind together in good solvent conditions for the polymer backbone ("spacer").[35,36] Phase separation of associative polymers is attributed to the enhanced attraction between polymer chains due to intermolecular interactions between sticky motifs.[35] This "sticker-and-spacer" model has recently inspired the design of short peptides containing hydrophobic residues linked together with polar amino acid spacers able to undergo simple coacervation at sub-millimolar concentrations.[17]

Complex Coacervation: In its simplest and most studied form, complex coacervation involves the complexation between two oppositely charged homo-polyelectrolytes. The optimal conditions for complex coacervation are met for an equimolar ratio of positive and negative charges, which can be identified by turbidity screening. The driving force of complex coacervation is attributed to the large entropy gain associated with the release of condensed counterions and rearrangement of water molecules when oppositely charged polymers form macroion pairs.[37] The enthalpic contribution of polyelectrolyte coacervation has often been reported to be endothermic[37–39] (due to the larger enthalpic cost to desolvate charge residues before ion pairing compared to the electrostatic interactions themselves[39]), although an exothermic signature has been observed in some cases.[38] There has been

an interest in recent years to develop complex coacervates using low molecular weight ions, such as oligopeptides and oligo-/mononucleotides,[14,15,97] metabolites,[40] or inorganic ions,[41] mostly motivated by the design of prebiotically relevant coacervate protocells. Compared to long polyelectrolytes, phase separation for shorter species is less favorable because the entropy gain associated to counterion release is counterbalanced by the large entropy loss of oligomers upon pairing.

Folded proteins may also undergo complex coacervation with oppositely charged polyelectrolytes[42,43] or proteins.[44] Protein/polyelectrolyte phase separation typically occurs on a relatively narrow pH range where the protein net charge and opposite polymer charge balance each other.[45,46] Charge anisotropy on the protein surface, such as the presence of charged patches, strongly influences the phase separation behavior,[47,48] which has been used to achieve selective protein coacervation.[47] Protein supercharging (e.g., via chemical modifications,[49] gene-encoded point mutations,[50] or addition of charged peptide tags[48]) has appeared as a promising strategy to favor protein/polyelectrolyte coacervation on broader experimental conditions, which could open perspectives to develop enzyme coacervates as catalytically active modules in synthetic cells.

2.2.2. Surfactant Coacervation

Small molecular amphiphiles have also been used to assemble coacervates. Polyelectrolyte/surfactant complex coacervation is favored by the formation of surfactant micelles that act as multivalent polyions,[25,51,52] but molecular amphiphiles may also undergo phase separation on their own via a process known as surfactant coacervation.[53,54] Three main types of surfactant coacervation have been reported. The clouding phenomenon refers to the phase separation of a single surfactant specie above a critical temperature (known as the cloud point) due to heat-induced micelle dehydration, reconfiguration (e.g., from spherical to cylindrical micelles), and short-range attraction. Phase separation is here attributed to the formation of an interconnected network of spherical or cylindrical (worm-like) surfactant micelles above the critical micelle concentration. Historically first observed for non-ionic surfactants, this clouding phenomenon has been extended to ionic amphiphiles, including saturated fatty acids.[16,19,55] The two other types of surfactant coacervation do not involve temperature changes but include phase separation of oppositely charged amphiphiles[56] (also known as catanionic systems, which can be regarded as a type of surfactant complex coacervation), driven by the entropy gain of counterion and water rearrangement; and sponge-like systems, where lipids self-assemble into a continuous L_3 phase (also called anomalous or sponge phase) consisting of interconnected lipid bilayers.[57,58] Unlike coacervates assembled from polyions, the main driving force of surfactant coacervation therefore lies in the hydrophobic effect and associated entropy gain upon release/rearrangement of water molecules.

2.2.3. Coacervation Driven by Specific Interactions

In order to achieve a finer control and selectivity over phase separation, an increasing number of studies is exploring new design strategies to produce coacervates based on specific interactions. Nucleotide hybridization has appeared as a particularly promising direction to achieve this purpose. The selectivity and thermal reversibility of Watson–Crick base pairing in DNA offer indeed a robust approach to achieve programmable network connectivity. In a seminal work, three-armed DNA junctions capable of self-assembling into dendrimer-like structures via pairing of sticky ends were developed.[59] Based on these results, multi-armed self-assembled DNA nanoparticles called DNA nanostars have been recently designed to undergo phase separation driven by nucleotide hybridization.[60,61] The formation of a DNA-dense phase requires the nanostars to exhibit a defined multivalency, which is achieved by introducing free sticky ends at the end of each arm. The latter develop attractive hybridization interactions below a critical temperature to produce a network of DNA nanostars. To avoid kinetic trapping into a gel or crystalline state, the nanostars further need to have some degree of internal flexibility, which is achieved using unpaired bases at specific locations.[61–64] These unpaired bases have been shown to be critical to allow nanostar mobility within the condensed phase. Excitingly, these DNA-based coacervate-like systems offer a great programmability since the DNA sequences can be precisely adjusted to achieve the desired material and functional properties.[65–69] An increasing number of studies are thus now geared toward demonstrating the potential of these systems as versatile modules in synthetic cells (see Section 4).

Beyond base pairing, protein recognition motifs orthogonal to those found in biological membraneless organelles have been exploited in a few in vivo studies to assemble artificial condensates. For instance, light-switchable condensates have been reported in cellulo based on reversible protein oligomerization under light illumination.[70–72] It is likely that such a design strategy based on specific protein recognition motifs will be exploited in future in vitro studies to engineer programmable coacervate artificial organelles in synthetic cells.

2.2.4. Biological Coacervates: The Peculiar Case of Biomolecular Condensates

Biomolecular condensates found in living cells are liquid-like membraneless organelles formed by phase separation between proteins and/or polynucleotides.[10,11] Compared to the coacervate systems described above, these condensates involve complex mixtures of chemically diverse components whose phase separation may be driven by nonspecific or specific interactions, or a combination of both.[73,74] Many biomolecular condensates involve intrinsically disordered proteins (IDPs) or proteins with intrinsically disordered regions (IDRs). IDPs or IDRs are amino acid sequences that do not adopt a defined 3D conformation but rather remain unfolded in physiological conditions, often due to the presence of low complexity domains enriched in a small number of charged or poorly hydrophobic amino acids. These domains include arginine/glycine-rich (RGG) motifs, as in the RNA helicases LAF-1[75] and Ddx4,[76] or in fused in sarcoma (FUS),[77] and prion-like domains with a [G/S]Y[G/N/A/S]AQ repeating sequence, as in FUS,[77–79] which develops cation–π interactions key in driving phase separation.

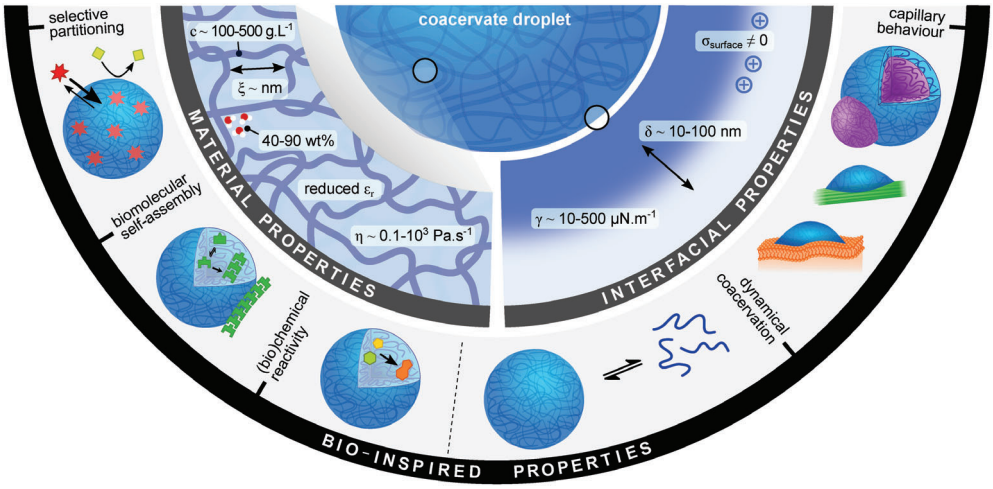

Figure 4. Schematic representation of the physicochemical properties and deriving bioinspired functions of coacervate microdroplets.

From a polymer physics viewpoint, IDPs can be described as sequence-defined chain-like macromolecules whose phase separation is driven by various nonspecific attractive interactions (electrostatics, cation–π, π–π stacking, dipole–dipole, H-bonding, etc.).[11,80,81] These interactions are not biospecific and are also found in the coacervates described above. Since IDPs carry both positive and negative charges and often contain sticky motifs (that can be as simple as single hydrophobic amino acids and as complex as folded β-sheets[82]), their phase separation behavior shares similarities with the coacervation of both polyampholytes[33] and associative polymers.[83]

Structurally defined binding domains may also favor protein phase separation with RNA or other proteins.[82,84,85] For instance, nucleophosmin (NPM1) forms a pentamer able to bind to ribosomal RNA via nucleic acid binding domains, but also to basic nucleolar proteins such as surfeit locus protein 6 (SURF6) or to other NPM1 pentamers.[86] In another example, multiple binding domains on the small ubiquitin-like modifier (SUMO) and SUMO-interacting motif (SIM) produce zipper-like filaments that assemble into a sticker-and-spacer-like system (where stickers are filament defects) driving phase separation.[87,88] Multivalency has also been shown to be critical for phase separation between repeats of the sarcoma homology 3 (SRC) domain and its proline-rich motif (PRM) ligand.[89]

Significantly, several studies have reconstituted biomolecular condensates in vitro, e.g., using purified recombinant proteins, paving the way to their integration in synthetic cells. Importantly, these condensates offer a level of programmability yet unmatched in conventional coacervates, e.g., in terms of selectivity over biomolecular recruitment or control over catalytic reactions. Harnessing the biochemical diversity and complexity of biological coacervates would thus provide new perspectives for the assembly of structurally and functionally elaborate synthetic cells.

2.3. Physicochemical Properties of Coacervate Droplets

The chemical diversity of coacervates highlighted in the previous section makes these systems highly versatile for the construction of synthetic cells. In this section, we briefly discuss some general material and interfacial properties of coacervate droplets (**Figure 4**), regardless of their chemical composition, and outline whenever relevant the system-specific properties of each type of coacervate.

2.3.1. Material Properties

Complex coacervates typically contain around 100–500 mg mL^{-1} of their constituents[90] but remain highly hydrated, with water contents comprised between 40%[91] and 90%[90,92] by weight. In rheology terms, complex coacervates behave as dense viscoelastic fluids that exhibit characteristics of liquids at long timescales, such as a spherical shape at equilibrium, deformability, fusion, and wetting of surfaces (all resulting from the existence of an interfacial tension, discussed below). More specifically, the viscosity of complex coacervates spans several orders of magnitude (≈0.1–10^3 Pa s^{-1}) depending on the chemical structure and length of the polyelectrolytes, and on the salt concentration or temperature.[93] These coacervates may exhibit an elastic response at shorter timescales (less than seconds), depending on the composition and salt concentration.[93] Gel-like or solid-like behaviors have also been reported at lower water content, i.e., when coacervate-forming species develop strong attractive interactions.[35,94,95] Local effects, such as polypeptide chirality[96] or polynucleotide rigidity[97,98] may also dictate the liquid versus solid behavior of polyelectrolyte complexes.

Surfactant coacervates composed of entangled worm-like micelles (often called "living polymers" due to their ability to easily break and reform) show similar viscoelastic properties to polymer solutions,[99–101] but readily reorganize under shear. In comparison, DNA nanostar coacervates have been reported to have a heterogeneous, clustered structure with high viscosities (≈10–100 Pa s^{-1}).[61] Importantly, salt had a contrary role on these DNA coacervates compared to polyelectrolyte complex coacervates: increasing the salt concentration resulted in the formation of more dense and more viscous phases due to stronger nucleotide hybridization upon salt-induced screening of DNA electrostatic repulsion.[61]

Due to the high chemical enrichment, a significantly reduced relative permittivity has been reported inside complex coacervates compared to water, reflecting a lower local polarizability.[14,102] As an example, an apparent dielectric constant of ≈40 (a value close to that of dimethylsulfoxide or acetonitrile) has been determined inside oligopeptide/mononucleotide complex coacervates.[14]

Despite relying on very diverse interactions, biomolecular condensates have been shown to share some material properties with complex coacervates,[13] such as liquid-like behavior, high biomolecular concentrations, (≈200–300 mg mL^{-1} reported for Ddx4 condensates[103]), low internal dielectric constant (a value of 45 has been reported for Ddx4 condensates[76]), and high viscosities (≈0.1–10^3 Pa s^{-1}).[104–106] Nonetheless, the biochemical complexity of these condensates confers them specific material properties. In particular, many condensates combine multiple types of interactions that underlie different self-assembly length scales and relaxation timescales.[85] Weak interactions ensure liquid-like behavior and dynamical properties to the condensates, but provide only poor structural and functional specificity. In comparison, strong interactions based on structurally defined binding motifs offer specificity but may result in slow dynamics and solidification. As a result, some biomolecular condensates are metastable and undergo maturation into more viscous fluids over time,[107] possibly evolving toward gel- or solid-like assemblies,[78] e.g., due to the formation of cross-β structures. Albeit challenging, the design of condensates with controllable transition from fluid versus dynamically arrested states[108] could be leveraged to regulate their functions in synthetic cells.

2.3.2. Interfacial Properties

Coacervate droplets behave as a liquid phase in another liquid phase. The coacervate–supernatant interfaces are therefore characterized by an interfacial tension, γ, with values typically comprised between 10 and 500 μN m^{-1}.[106,109–112] This surface tension correlates with the interaction strength between phase separating species. Therefore, for complex coacervates, the surface tension decreases when the salt concentration increases, and is higher for longer polyelectrolytes compared to shorter ones.[109] By contrast, the surface tension of DNA coacervates has been shown to increase with the salt concentration due to stronger pairing interaction at higher ionic strength.[61] Due to the small value of the interfacial tension, the balance of Laplace pressure with shear stresses due to external flows leads to large deformations of the coacervates (even at moderate external flows). In addition, the low interfacial tension is associated to a large interfacial thickness δ (since γ scales as $k_B T/\delta^2$) compared to water/oil systems. For instance, the computed density profile at the interface of poly-L-lysine (pLys)/poly-L-glutamic acid (pGlu) coacervates showed a gradient of polypeptides spanning ≈20 nm.[113] Similar values have been computed for biomolecular condensates assembled from proteins containing prion-like low complexity domains, and attributed to the expanded conformation of proteins and their perpendicular orientation at the interface.[114]

In addition, coacervate droplets may exhibit a non-neutral net surface charge. This is particularly true for surfactant and DNA nanostar coacervates that are assembled from a single charged specie. For complex coacervates, charge neutrality is usually targeted to maximize the volume fraction of the coacervate phase; the interior of coacervates is therefore neutral but some excess surface charge may persist. The net surface charge can be tuned from positive to negative by varying the ratio of positive-to-negative charges. The presence of charges at the interface kinetically stabilizes the coacervate and reduces the coarsening by preventing coalescence: smaller coacervate droplet dispersions are therefore observed in conditions far from electroneutrality.[115] Similarly, excess surface charges have been reported in biomolecular condensates assembled from FUS, and shown to decrease their fusion propensity.[116]

We will see in Section 5 how the peculiar interfacial properties of coacervates, including their low surface tension, large interfacial thickness, and excess surface charge have strong implications on their templating capability.

3. Bioinspired Properties of Coacervate Droplets

Deriving from their physicochemical properties, coacervate microdroplets exhibit a range of bioinspired functional properties (Figures 4 and 5) outlined in this section. These bioinspired properties, mostly inspired by the functions of membraneless organelles in living cells,[117] constitute the basis for the construction of coacervate-based synthetic cells.

3.1. Partitioning and Molecular Transport

3.1.1. Equilibrium Partitioning

A key property of coacervate microdroplets is their ability to spontaneously sequester various solutes (usually called "guest" or "client" species), including inorganic ions,[118] small molecules,[119] and bio-macromolecules.[118,120] This partitioning depends on the combination of a number of factors, including noncovalent interactions with scaffold coacervate components,[121] the reduced polarity inside droplets that favors the uptake of hydrophobic molecules,[102] and the characteristic mesh size of the coacervate matrix that may prevent the entry of larger or more rigid solutes[76,122] (**Figure 5**a). At thermodynamic equilibrium, the distribution of guest species within coacervate droplets relative to the supernatant is dictated by their chemical potential in these two phases, which is characterized in diluted solutions by a partition coefficient, K, namely, the ratio of solute concentration in the coacervate versus supernatant phases. Experimentally, the partition coefficient can be accessed via spectroscopy measurements (on macroscopically phase-separated samples) or confocal fluorescence microscopy (on individual droplets). It should be noted that this ideal thermodynamic description does not take into account saturation effects[123] or the possible replacement of coacervate components by charged solutes. It is also unclear how nonequilibrium conditions (e.g., in chemically fueled or reactive coacervate droplets, see below) may affect the partitioning of species.

In addition, at thermodynamic equilibrium, sequestered solutes still diffuse across the coacervate interface into the supernatant, a process that is kinetic- or diffusion-limited, and retain a

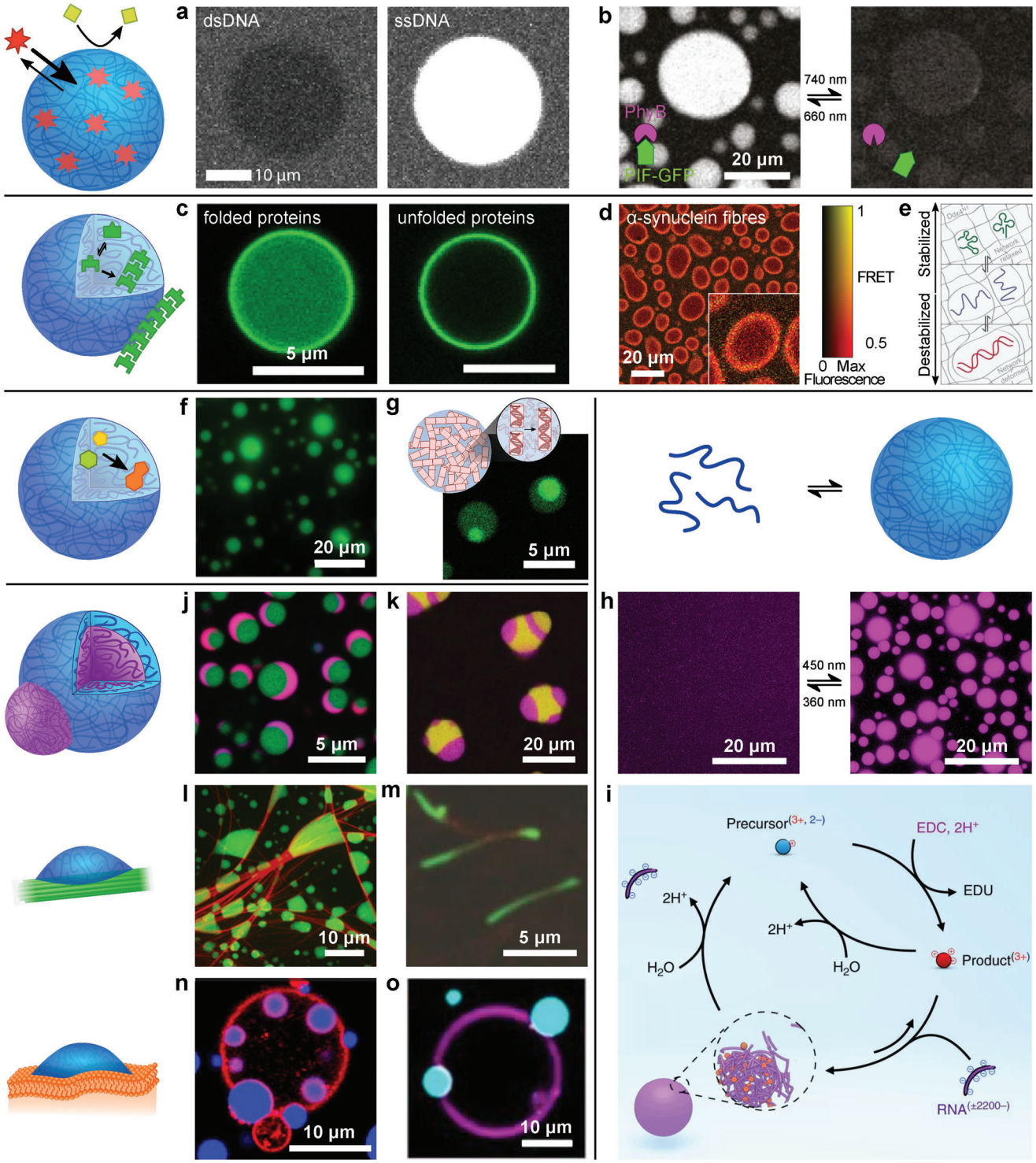

Figure 5. Examples of bioinspired properties of coacervate droplets. a) Selective exclusion and sequestration of dsDNA and ssDNA, respectively, from Ddx4 condensates. Reproduced under the terms of the CC-BY license.[76] Copyright 2015, The Authors. Published by Elsevier Inc. b) Light-switchable capture and release of fused green fluorescent protein (GFP)–phytochrome interacting motifs (PIFs) from lipid sponge coacervates functionalized with the photoreceptor phytochrome B (PhyB). Reproduced with permission.[58] Copyright 2020, PNAS. c) Sequestration of bovine serum albumin within PDDA/PAA coacervate droplets, and interfacial adsorption upon urea-mediated unfolding. Reproduced with permission.[134] Copyright 2016, American Chemical Society. d) Interfacial aggregation of FRET-labeled α-synuclein on pLys/pGlu coacervates. Reproduced under the terms of the CC-BY license.[139] Copyright 2022, The Authors. Published by American Association for the Advancement of Science. e) Ddx4 condensates destabilize extended and rigid nucleic acid duplexes but favor compact single chains due to the minimal distortion of the protein network. Reproduced with permission.[141] Copyright 2016, Nature Publishing Group. f) Fluorescence associated to ribozyme-mediated cleavage of RNA in pLys/CM-dex coacervates. Reproduced under the

certain degree of mobility within the coacervate phase.[123] Small molecules generally diffuse freely through the coacervate matrix via Brownian motion, while larger molecules may experience a restricted diffusion due to steric hindrance, e.g., when the size of molecules is larger than the typical mesh size of the matrix. Fluorescence recovery after photobleaching (FRAP) is routinely used to determine the diffusion properties of guest solutes. Molecular transport within coacervates is also influenced by interactions with the coacervate components. Therefore, even small molecules can experience a subdiffusive transport in coacervates, as reported in a study where a molecular rhodamine dye was shown to exhibit non-Fickian transport in protein/DNA coacervates due to cation–π interactions with proteins in the coacervate matrix.[124]

3.1.2. Selective and Switchable Partitioning

Achieving selective and/or switchable partitioning in coacervates would be highly desirable to control the localization of molecules in synthetic cells. Studies have reported selective solute sequestration based on electrostatic interactions, including selective protein coacervation[47,125,126] or protein partitioning in complex coacervates.[127,128] However, fine control over the exact level of solute recruitment and release remains highly challenging with nonspecific interactions. To overcome this limitation, recent efforts have been geared toward selectively addressing solutes to coacervate droplets using specific interactions. For instance, proteins bearing a histidine hexamer (His_6) tag were shown to be efficiently sequestered, while still remaining mobile, within lipid-[58] or polymer-based[129] coacervates functionalized with Ni^{2+}–nitrilotriacetic acid (NTA). Biotin–streptavidin binding was also used to capture biotinylated double-stranded DNA (dsDNA) strands within lipid-based coacervates functionalized with biotinylated lipids in the presence of streptavidin.[58] In another example, benzylguanine-modified phospholipids were incorporated in lipid sponge coacervates and shown to covalently capture SNAP-tag fusion proteins.[130] Other works used nucleotide hybridization in DNA nanostar coacervates to selectively sequester complementary dsDNA[131] or ssDNA[132] strands, as well as protein–DNA conjugates.[133]

Excitingly, the use of specific interactions opens the possibility to achieve controllable uptake and release of guest species. In an illustrative example, Devaraj and co-workers demonstrated reversible light-mediated protein capture and release in lipid sponge coacervates based on a protein photoreceptor able to switch between a binding and nonbinding conformation with light (Figure 5b).[58] Protease-mediated cleavage of terminal His_6-tags has also been exploited to trigger protein release from NTA-containing coacervates.[129] Controllable release of DNA strands or protein–DNA conjugates was last demonstrated in DNA coacervates using light[132] or DNA strand displacement reactions,[133] respectively. Such a dynamical control over the localization of functional biomolecules opens perspectives for the coordination of different processes in synthetic cells. A higher level of control would require the use of different, orthogonal interactions to regulate the localization of multiple species independently.

3.2. Biomolecular Self-Assembly

3.2.1. Protein Stability, Oligomerization, and Aggregation

Coacervate droplets provide a distinct physicochemical environment to the proteins they concentrate by partitioning, which may affect their stability. In a study, the conformation of globular proteins, including bovine serum albumin, carbonic anhydrase, and α-amylase, was studied in polydiallyldimethylammonium chloride (PDDA)/polyacrylic acid (PAA) complex coacervates.[134] Native proteins were shown to be sequestered within coacervate droplets while urea-unfolded proteins tended to be accumulated at the droplet interface (Figure 5c).[134] Importantly, circular dichroism measurements revealed that the coacervate phase increased the thermodynamic stability of proteins, which was attributed to macromolecular crowding and excluded volume effects[134] (which favors more compact (folded) protein conformations). Interestingly, lipid sponge droplets were shown to allow the reconstitution of transmembrane proteins, thanks to the bilayer environment within the droplets that ensured correct protein folding and membrane insertion.[58] It is also worth mentioning that a few other studies are exploring the role of coacervation on minimal peptide folding from an evolutionary perspective, which could also provide insight into the interplay between coacervation and protein stability.[135,136]

According to the law of mass action, the high local concentration of proteins within coacervates can also promote protein oligomerization and aggregation. For instance, a 50-fold enhancement in actin filament assembly rate was reported in complex coacervates.[137] The interface of complex coacervate has also been reported to play a critical role in promoting the formation of actin filaments[138] or α-synuclein (αSyn) fibrils (Figure 5d).[139] Yet, other examples have shown that the coacervate interface could play a protective role against protein aggregation during folding via the sequestration of partly folded

terms of the CC-BY license.[156] Copyright 2018, The Authors. Published by Springer Nature. g) Enzyme-free oligonucleotide ligation in DNA/azobenzene cation coacervates gives rise to the formation of multiphase coacervates by spontaneous self-sorting of long polynucleotides. Reproduced under the terms of the CC-BY-ND-NC license.[144] Copyright 2023, The Authors. Published by Springer Nature. h) Light-switchable coacervation between dsDNA and azobenzene cations. Reproduced with permission.[168] Copyright 2019, Wiley-VCH. i) Chemical reaction cycle coupled to RNA/peptide coacervate formation and decay. Reproduced under the terms of the CC-BY license.[183] Copyright 2020, The Authors. Published by Springer Nature. j) Multiphase complex coacervates produced with polyallylamine hydrochloride (PAH), protamine, PAA, and pGlu. Reproduced with permission.[188] Copyright 2019, American Chemical Society. k) Multiphase DNA nanostar coacervates. Reproduced with permission.[65] Copyright 2020, American Chemical Society. l) Tau protein condensate wet microtubules. Reproduced with permission.[201] Copyright 2017, Cell Press. m) Wetting of pLys/RNA coacervates (green) on FtsZ fibrils (red). Reproduced with permission.[202] Copyright 2018, Springer Nature. n) Partial engulfment and endocytosis of PDDA/ATP coacervates in negatively charged liposomes. Reproduced under the terms of the CC-BY license.[204] Copyright 2022, The Authors. Published by American Chemical Society. o) Partial wetting of glycidin condensates on zwitterionic giant unilamellar vesicles (GUVs). Reproduced with permission.[206] Copyright 2023, Springer Nature.

aggregation-prone intermediates.[134] Similarly, a significantly slower kinetics of αSyn aggregation has been observed in coacervates due to the sequestration and stabilization of the monomeric form of the protein.[139] A deeper understanding of the interplay between protein sequestration, stability, oligomerization, or aggregation and coacervate properties could open perspectives for the design of droplets capable of regulating cytoskeleton nucleation and growth or acting as protein quality control modules in synthetic cells. Progress in this direction will benefit from knowledge gained on the fundamental role of biomolecular condensates in regulating both physiological and pathological protein aggregation.[140]

3.2.2. Polynucleotide Hybridization

Nucleotide pairing in double-stranded DNA is also affected by coacervates. In a study, coacervates assembled from disordered proteins with sequences similar to Ddx4 were shown to destabilize oligonucleotide duplexes (Figure 5e),[141] as determined via Förster resonance energy transfer (FRET). This observation was interpreted in terms of coacervate mesh size, which favored the melting of rigid dsDNA into flexible ssDNA to avoid distortion of the underlying coacervate structure, and favorable interactions between flexible nucleic acids on ssDNA and coacervate-forming proteins. These droplets were further shown to stabilize folded single-stranded oligonucleotide structures, which was explained by the ease of compact strands to fit into the mesh-like structure of coacervates over extended conformations.[141] Nucleic acid hybridization in RNA was also found to be affected inside peptide-based coacervates, and was shown to be all the more reduced when longer polypeptides were used.[15] In another recent example, dsRNA dissociation equilibria were investigated in more complex environments where multiple peptide-based coacervate phases coexisted to produce multiphase coacervates.[142] Results showed that single- and double-stranded RNA strands preferentially accumulated in different phases of the same droplet, with one phase having a more destabilizing effect than the other. Deciphering the mechanisms underlying (de)stabilization of nucleic acid duplexes in coacervates could open perspectives for the design of functional modules with helicase-like activity in synthetic cells.

3.2.3. Other Supramolecular Self-Assemblies

Last, coacervate droplets may also guide other types of supramolecular self-assembly processes. For instance, the up-concentration of oligonucleotides upon complex coacervation with pLys[143] or azobenzene cations[144] was shown to promote their end-to-end stacking into longer physical polynucleotides. Interestingly, this arrangement of oligonucleotides promoted the emergence of a liquid crystalline coacervate phase on a small range of salt concentrations where partial charge screening provided sufficient fluidity to the droplets.[143–145] In other notable examples, synthetic amphiphilic peptides,[146] dipeptides,[147] or tripeptides[148] have been reported to form fibers due to their accumulation within coacervates or at their interface. These studies generalize the role of coacervates in regulating self-assembly processes, which could be exploited for the construction of synthetic cytoskeleton-like fibers in synthetic cells.[149]

3.3. Chemical Reactivity

Biomolecules accumulated within coacervate droplets remain mobile, a prerequisite to ensure dynamic molecular interactions and enzyme activity. Therefore, several enzymes have been shown to retain their activity within coacervate droplets, including carbonic anhydrase,[134] horseradish peroxidase,[150] uricase,[151] protease,[58] actinorhodinpolyketide synthase,[152] or even more complex enzyme mixtures for in vitro transcription-translation.[58,153] In many cases, enzyme reactions are simply reported qualitatively via the production of a fluorescent product. From a more rigorous viewpoint, coacervate droplets impact both the kinetics and thermodynamics of enzyme reactions.[121] As far as the thermodynamics is concerned, the reduced internal permittivity of coacervates, together with interactions with coacervate components and macromolecular crowding effects, can affect the energy landscape of the reaction,[121] for instance, by altering the conformation of enzymes (and therefore their affinity for their substrate or the structure of intermediate states).

From a kinetics perspective, a rate enhancement is expected if the enzyme and its substrate are both accumulated and colocalized in the droplets. Excluded volume effects in the coacervate matrix can also result in accelerated reactions (enzyme and substrate meet faster as they have a lower volume to explore). However, the high viscosity of the coacervate matrix, together with interactions between the coacervate components, competes with the above phenomena by restricting protein diffusion and leads to a reduced kinetics. Similarly, the accumulation of product in the coacervate droplets may result in a lower kinetics due to product inhibition. Therefore, the exchange of material between coacervate droplets results in "open" compartments, and their surroundings should not be neglected. Yet, in most reported studies, a detailed analysis of the kinetics of enzyme reactions and of enzyme, substrate, and product partitioning is lacking.

In a seminal example, Beneyton et al. investigated the catalytic activity of formate dehydrogenase within single carboxymethyl dextran (CM-dex)/PDDA and pLys/adenosine triphosphate (ATP) complex coacervates assembled in water-in-oil microfluidic droplets.[154] An increase in initial reaction rate was observed compared to the absence of coacervates, which was attributed to the accumulation (and therefore colocalization) of the enzyme and its nicotinamide adenine dinucleotide (NAD^+) cofactor in the coacervates. Remarkably, the initial reaction rate was also higher in the emulsion droplets, where the coacervate and supernatant phases coexist, compared to the bulk coacervate phase. Based on partitioning measurements, this increased kinetics was hypothesized to result from a shift in the reaction equilibrium due to the removal of the product from the coacervate droplet into the surrounding aqueous phase.[154] This approach could serve as a general platform to quantify the kinetics of other enzyme reactions.

Other studies have investigated ribozyme-catalyzed reactions including template-directed RNA polymerization,[155] RNA cleavage[156,157] (Figure 5f), and RNA ligation,[158] in different complex coacervate systems. Notably, strong electrostatic

interactions between RNA and polycations were shown to reduce ribozyme activities.[155,157] Addition of excess polyanions to compete with unfavorable RNA–polycation interactions was shown to restore, and even enhance, ribozyme-mediated RNA cleavage.[157] In another study, the accumulation of magnesium cations together with a high RNA fluidity within coacervates were identified as key factors to favor ribozyme activity in phase separated droplets.[158] Phase separation of ribozymes with pLys was also shown to activate RNA ligation or cleavage in conditions where the enzyme was otherwise inactive.[159] Significantly, the equilibrium was shifted toward RNA ligation rather than cleavage within such coacervates, which was attributed to the higher RNA concentration in the droplets. Altogether, these studies inform us on the multiple roles of coacervates in modulating enzyme reactions. Notably, beyond the upconcentration and colocalization of reactants, the local microenvironment created by the coacervate matrix is found to play a significant role on enzyme activities.

More complex reactions such as gene-directed translation and transcription have also been investigated in coacervate droplets, with examples showing enhanced transcription rates[160] and protein expression,[153] which was attributed to macromolecular crowding effects together with the locally high concentration of biomolecular components.

Last, recent studies have started exploring simpler chemical reactions in coacervates (without enzymes), including aldol reactions and hydrazone formation,[17] redox conversions,[40] amide bond formation,[41] and oligonucleotide polymerization via carbodiimide-activated esterification.[144] In the latter example, an enhanced reaction kinetics and yield were observed and attributed to a combination of nucleic acid liquid crystal ordering, high local concentrations of reactive groups, and low water activity within coacervates, favoring esterification over hydrolysis.[144] Surprisingly, oligonucleotide polymerization resulted in the formation of coacervate subdomains via self-sorting of long polynucleotides (Figure 5g). These studies highlight the potential of coacervates to favor otherwise slow or unfavorable chemical reactions, which could be used for metabolic reactions in synthetic cells. A deeper understanding of reactions in coacervates will benefit both from studies on the effect of biomolecular condensates on biochemical reactions in cells and from studies of reactions confined in other types of microenvironments.[161–163]

3.4. Dynamical Phase Separation

There has been a growing interest in recent years to design dynamic coacervate droplets able to reversibly form and dissolve. Such a dynamical phase separation represents a promising approach to activate processes in synthetic cells by controlling the sequestration of functional solutes within coacervates and their release upon droplet dissolution.

3.4.1. Stimuli-Responsive Coacervates

The simplest way to trigger the formation or dissolution of coacervates is to use stimuli-responsive systems. Complex coacervates assembled from weak polyacids or polybases (i.e., polyelectrolytes whose ionizable groups are partially ionized in water) are readily sensitive to pH and are formed or dissolved by altering the charge density on the polyions. For instance, pLys/ATP coacervates are disrupted at high and low pH values due to neutralization of amine groups on pLys or of phosphate groups on ATP, respectively.[14] Physical stimuli such as temperature also readily induce simple coacervation of LCST-like polymers, such as elastin-like polypeptides[29,30] or ssDNA,[30,31] but also surfactant coacervation via the clouding phenomenon.[16,19,55,56] Examples of temperature-sensitive complex[164–167] and biological[76] coacervates have also been reported, including LCST-like[164,165] or UCST-like[76,166,167] behaviors.

Optical control of associative liquid–liquid phase separation has emerged in recent years as an enticing approach to control coacervate formation and dissolution with a finer spatiotemporal control. In a pioneering example, cationic azobenzene photoswitches have been reported to form photoswitchable complex coacervate with dsDNA due to light-actuated *trans–cis* azobenzene isomerization[168,169] (Figure 5h). Importantly, selective coacervate disassembly was demonstrated by irradiating with UV light a single droplet in a population of coacervates, illustrating the potential of light to spatially regulate phase separation.[168] Since then, other examples of photoswitchable coacervates based on azobenzene photoswitches have been reported, including with oligonucleotides,[144] polysaccharides,[170,171] and azobenzene-conjugated ssDNA,[172] illustrating the generality of this approach. Light has also been used to regulate the phase separation of proteins, either irreversibly using photocleavable groups,[173] or reversibly using light-switchable protein oligomerization.[70–72]

3.4.2. Active Growth and Dissolution of Coacervates

Many regulatory processes of biomolecular condensates in living cells rely on active processes, such as protein or RNA synthesis or degradation, or posttranslational modifications such as phosphorylation or methylation. Reproducing such self-driven behaviors is an area of active research, which builds upon the design of coacervate systems that form and/or dissolve based on energy-consuming processes. These systems present the advantage of being self-regulated (they do not require an external intervention to switch from one state to the other), which could be used to achieve autonomous control over functions in synthetic cells.

The active formation and/or dissolution of coacervate can be achieved using enzyme reactions that alter the charge or concentration of phase separating species, e.g., via phosphorylation/dephosphorylation reactions,[174–176] polynucleotide synthesis[177–179] or ligation,[180] or proteolytic cleavage of solubilizing tags;[181] or reactions that induce a change in the environmental conditions, e.g., a change in pH.[46,150] Chemical reactions have also been used to actively form coacervates[182] and push them out of equilibrium via formation/dissolution equilibria[183,184] (Figure 5i). Under such active processes, transient coacervate assembly or transient multiphase organization has been observed.[46,175,183,184] Nonspherical coacervate shapes have also been reported for coacervates actively formed by enzyme-driven elongation of RNA strands.[179] Interestingly, when competing interactions that synthesize and degrade phase separating coexist, theoretical studies predict that shape instabilities can lead to droplet division.[185] If realized experimentally,

these processes could be used to achieve energy-driven organelle growth and division in synthetic cells as observed in living cells.

3.5. Capillary Behavior

The existence of an interfacial tension at coacervate/supernatant interfaces generates capillary behaviors that are general to liquid-like systems. Such phenomena, also observed in cellulo for biomolecular condensates,[186] can be exploited to organize coacervates at other liquid or solid interfaces, as discussed below.

3.5.1. Multiphase Organization

The wetting properties of coacervates can manifest at liquid–liquid interfaces to produce multiphase coacervates[187–193] (Figure 5j,k). When two immiscible coacervates (1 and 2) coexist, three surface tensions are defined: one between the two coacervate phases, γ_{12}, and two between each individual coacervate and the supernatant, γ_1 and γ_2. Depending on the relative values of these interfacial tensions, complete wetting, partial wetting, or nonwetting occur. Complete wetting is observed when $\gamma_{12} < \gamma_1$ and $\gamma_{12} < \gamma_2$, and may result in full engulfment of one droplet by the other, provided a sufficient difference in coacervate size is met. In this case, coacervate droplets with higher interfacial tension are more likely to be engulfed. Partial wetting is expected when $\gamma_{12} > \gamma_1$ and $\gamma_{12} > \gamma_2$, and nonwetting may occur when $\gamma_{12} \geq \gamma_1 + \gamma_2$. Multiphase complex coacervates have been reported to form regardless of the order of addition of polyelectrolytes,[188] indicating that it is an equilibrium phenomenon. Moving toward more programmable systems, a multiphase organization has been realized by designing specific protein sequences[194,195] or DNA-motifs,[65,196] as well as by rationally synthesized zwitterionic polymers.[13] These approaches expand the methodological toolkit to control the mesoscopic properties of multiphasic coacervate droplets.

From a functional viewpoint, many membraneless organelles also exhibit a multiphase hierarchical architecture in living cells that enables them to execute sequential reactions with efficient coordination. The nucleolus is the most prominent example of such a functional organization where the different layers sequentially participate to ribosome biogenesis.[197] Inspired by these biological systems, and taking advantage of the ability of different coacervate phases to sequester guest molecules selectively, the spatial arrangement of cascade enzyme reaction has been demonstrated in hierarchical coacervates.[191,198] Furthermore, since multiphase coacervates exhibit dissimilar densities due to different critical salt concentrations, selective dissolution or condensation of the outer coacervate layer in response to enzyme reactions has been achieved[46,199] as a first step toward more complex dynamical behaviors.

3.5.2. Wetting of Soft Surfaces

Wetting has also been evidenced at coacervate–solid interfaces, including protein fibers and lipid bilayers. Remarkably, coacervate droplets were reported in a few examples to deform in the presence of semiflexible cytoskeletal protein filaments, including actin,[200] tubulin[201] (Figure 5l), and Filamenting temperature-sensitive mutant Z (FtsZ)[202,203] (Figure 5m), a bacterial homologue of tubulin. These shape changes have been attributed to the low interfacial tension of coacervates (and therefore low energy cost associated to the increase of their surface-to-volume ratio), together with capillary forces that induced the coacervate phase to wet the protein fibers. Interestingly, such capillary forces have also been evidenced between condensates and fibers in living cells.[186,201] The interplay between coacervation and cytoskeleton self-assembly will be discussed more in detail in Section 5.

In addition, similar to condensates in living cells,[186] coacervate droplets wet lipid bilayers, as very recently evidenced in vitro upon mixing different types of coacervates, including complex DNA nanostars and biological coacervates, with giant unilamellar vesicles (GUVs)[196,204–209] (Figure 5n,o). This wetting behavior has been shown to perturb the organization of lipids within bilayers, either producing pores[195] or increasing lipid packing.[205] Remarkably, capillary forces on soft and deformable lipid bilayers generate elastocapillary effects that have been reported to result in significant membrane deformations, such as fingering[206] and nanotube formation.[207–209] In a striking example, complete engulfment of coacervate droplets adsorbed on the external surface of GUVs has been observed, driven by charge interactions with lipids, ultimately leading to the formation of lipid-coated coacervates within vesicles in a process reminiscent to endocytosis[204] (Figure 5n). Such an approach demonstrates a possible route to achieve cargo transfer across membranes.

4. Coacervates as Artificial Organelles in Synthetic Cells

Inspired by in vivo biomolecular condensates, and building upon their bioinspired functions, coacervate microdroplets have started been integrated as simple forms of membraneless organelles within membrane-bounded compartments, including water-in-oil emulsion droplets, GUVs, polymersomes, and proteinosomes. In this section, we first categorize the approaches that have been used to build nested coacervate-in-compartment structures, then illustrate the functions that have been realized with such proto-organelles.

4.1. Assembly of Coacervate Droplets within Membrane-Bounded Compartments

The construction of coacervate-in-compartment systems follows three main strategies: coassembly, in situ triggered coacervation, and coacervate encapsulation (**Figure 6**).

4.1.1. Microfluidics-Assisted Compartment Coassembly

Microfluidics is highly attractive for the bottom-up construction of synthetic-cell-like compartments with a precise control of self-assembly in both time and space.[210] Droplet-based microfluidics provides a straightforward route to the coassembly of large populations of monodisperse and stable coacervates within membrane-bounded microcompartments, including water-in-oil

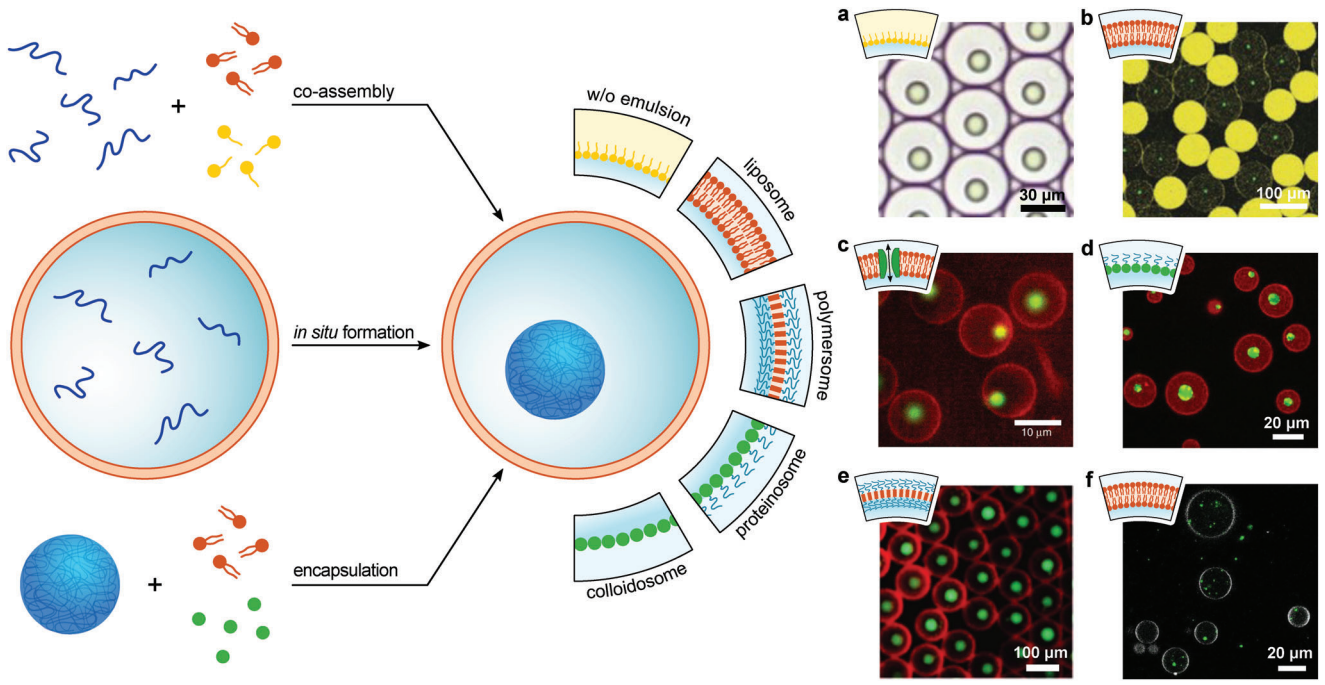

Figure 6. Construction of organelle-like coacervates in membrane-bounded compartments. Three strategies are used for the assembly of nested coacervate-in-compartment structures: i) the microfluidics-assisted coassembly of coacervates and compartments; ii) the in situ formation of coacervates, triggered by a stimulus, the outer addition and diffusion of a phase separating species or its enzyme-mediated synthesis; iii) the encapsulation of preformed coacervates by emulsification. a) pLys/ATP coacervates produced by microfluidics in water-in-oil (w/o) emulsion droplets. Reproduced with permission.[154] Copyright 2020, Wiley-VCH. b) Spermine/poly(uridylic acid) (polyU) coacervates assembled by microfluidics in GUVs (the large bright yellow droplets are the dewetted excess oil droplets). Reproduced under the terms of the CC-BY license.[215] Copyright 2017, The Authors. Published by Wiley-VCH. c) pLys/ATP coacervates produced in liposomes via encapsulation of pLys followed by the external addition of ATP and its diffusion through α-hemolysin pores. Reproduced under the terms of the CC-BY license.[178] Copyright 2018, The Authors. Published by Springer Nature. d) PDDA/succinylated dextran (Su-dex) coacervates formed in situ within proteinosomes after removal of salt. Reproduced with permission.[220] Copyright 2021, The Royal Society of Chemistry. e) PAH/ATP coacervates assembled within polymersomes after in situ conversion of adenosine diphosphate (ADP) into ATP by pyruvate kinase. Reproduce under the terms of the CC-BY license.[219] Copyright 2022, The Authors. Published by Springer Nature. f) Terpolymer-stabilized complex coacervates encapsulated within GUVs by an inverted emulsion technique (droplet transfer method). Reproduced under the terms of the CC-BY license.[225] Copyright 2022, The Authors. Published by American Chemical Society.

(w/o) droplets or liposomes.[211] In a study, the coencapsulation of polyanions and polycations in w/o droplets using a flow-focusing junction produced highly monodisperse coacervates within each emulsion droplet[154] (Figure 6a). The authors showed fine-tuning of coacervate size by adjusting the initial concentrations of polyions using pLys/ATP, PDDA/ATP, CM-dex/pLys, and CM-dex/PDDA systems. Other studies used a similar approach to encapsulate peptide/polyanion[212] or protein condensates[213,214] in w/o droplets, and subsequently analyzed the dynamics of liquid–liquid phase separation[212,213] or determined phase diagrams by using the multiplexing capabilities of droplet-based microfluidics.[214]

Although water-in-oil droplets do not recapitulate key features of cellular compartments such as an external aqueous environment, these examples demonstrate the potential of microfluidics for the coassembly of compartments and coacervates. Moving toward more biologically relevant compartments, a coaxial-microcapillary-based device for double-emulsion formation was used to coassemble monodisperse coacervates, including ATP/pLys, poly(uridylic acid) (polyU)/spermine, or coenzyme A/polyarginine, in liposomes[215] (Figure 6b). In this work, polycations and polyanions were loaded using core–shell inlets into double emulsion droplets. As the solvents evaporated, the double emulsion templates underwent a dewetting transition to generate uniform unilamellar liposomes in which concomitant phase separation led to single monodisperse coacervates.

4.1.2. Triggered In Situ Coacervation

Alternative methods to prepare coacervate-in-compartment structures rely on a sequential approach where membrane-bounded compartments are first assembled followed by the in situ formation of coacervates. Three main strategies have been devised based on passive molecular diffusion across membranes, stimuli-responsive coacervates, or in situ enzyme-based reactions.

Complex coacervates involve two oppositely charged species, therefore their formation can be induced within compartments by first encapsulating one of the components (during compartment self-assembly), then adding the second one to the external milieu and letting it diffuse through the membrane. This strategy has been easily implemented in proteinosomes, since their highly porous shell allows the diffusion of small species while

retaining longer polymers.[170,216] A similar approach has also been applied to liposomes, but unlike proteinosomes, diffusion of charged species across lipid bilayers required addition of membrane pores. In an example, pLys was first encapsulated within liposomes produced by microfluidics, then α-hemolysin pores embedded in the membrane allowed diffusion of ATP added to the external milieu, ultimately resulting in pLys/ATP coacervation within the liposomes[178] (Figure 6c).

Stimuli-responsive coacervation has been employed as another straightforward approach to induce in situ phase separation: in this case, coacervate-forming species are first encapsulated in membranous compartments under conditions where they do not phase separate, then phase separation is triggered by a change in the environmental conditions. In two different examples, pLys and ATP were coencapsulated inside lipid vesicles at a pH above the pK_a of pLys[217] or below the pK_a of the terminal phosphate of ATP,[218] where the deprotonated form of pLys or the protonated form of ATP was unable to interact with ATP or pLys, respectively, so that coacervation did not occur. A decrease or increase in the external pH to a value below the pK_a of pLys or above the pK_a of ATP, respectively, was then used to trigger pLys/ATP coacervation inside GUVs, which was possible because phospholipid membranes exhibit a sufficient proton permeability to equilibrate a transmembrane pH gradient. Following a similar strategy, pH-induced poly(allylamine hydrochloride) (PAH)/ATP complex coacervation was achieved within polymersomes in which membrane was engineered to be permeable to protons.[219] In another example, PDDA and succinylated dextran were coencapsulated in proteinosomes in the presence of a high salt concentration to screen electrostatic interactions, then in situ coacervation was triggered by the diffusion of salt across the porous protein shell[220] (Figure 6d). Compared to chemical cues, physical stimuli are readily transmitted through membranes without careful design of the membrane permeability and may appear as a simpler approach to induce in situ phase separation. Examples include temperature-induced ELP-based[221–223] and polyU/spermine[215] coacervation inside polymersomes and GUVs, respectively; and light-triggered biomolecular condensation and complex coacervation in water-in-oil emulsion droplets[173] and GUVs,[224] respectively.

Last, in situ biochemical reactions, including polynucleotide synthesis,[178] biomolecule phosphorylation[219] (Figure 6e), or proteolytic cleavage,[181] have been employed to trigger the formation of coacervates within compartments. These approaches open perspectives for the design of self-regulated dynamical organelle formation within synthetic cells.

4.1.3. Encapsulation of Preformed Coacervates

Although challenging due to possible interferences between coacervates and membrane components, the direct encapsulation of discrete coacervate microdroplets within liposomes[225] or Pickering emulsions[226] has been recently reported. In an illustrative example, Song et al. used an inverted emulsion method to encapsulate preformed coacervate microdroplets within liposomes[225] (Figure 6f). Terpolymer-stabilized coacervates prepared by oppositely charged amyloses were first enclosed within lipid-stabilized water-in-oil droplets via emulsification. This emulsion was then layered on top of an aqueous phase, and droplet transfer across the lipid-coated oil/water interface by centrifugation led to liposome formation with encapsulated coacervates. It is likely that the neutral polymer coating on coacervates together with the use of PEGylated lipids helped in avoiding direct interactions between the coacervate matrix and lipids during the assembly of liposomes. Interestingly, the endocytosis-like coacervate engulfment by GUVs discussed in Section 3 could also provide a promising approach to assemble membrane-stabilized coacervate organelles within vesicles.[204]

4.2. Functions of Encapsulated Organelle-Like Coacervates

Building on their bioinspired properties, coacervates have recently started being used as spatiotemporal organizers of synthetic cell content. We exemplify in this section the functions that have been demonstrated using coacervate droplets encapsulated within membrane-bounded compartments (**Figure 7** and **Table 1**). Albeit still nascent, these studies mark the first milestones toward the integration of various specialized membraneless-organelle-like modules able to perform complex, coordinated tasks within synthetic cells.

4.2.1. Switchable Condensation

Based on the capacity of some coacervates to reversible form and dissolve in response to a stimulus, various studies have demonstrated dynamic organelle assembly and biomolecular localization within membrane-bounded compartments, including water-in-oil emulsion droplets, GUVs (Figure 7a), and proteinosomes, e.g., in response to temperature,[194,215,221–223] pH,[178,217,218] chemical,[212] and enzyme[170,178,181,219] reactions or light.[170,173] For instance, temperature-responsive polyU/spermidine coacervates were used to demonstrate storage and release of fluorescently labeled dsDNA strands within liposomes.[215] In another study, Mu et al. encapsulated light- and pH-responsive coacervates within proteinosomes to demonstrate simple forms of Boolean logic gates:[170] as an example, a NAND logic gate was developed based on β-galactosidase- and glucose-oxidase-loaded coacervates, where the input of both lactose and oxygen was required to reduce the solution pH, resulting in the negative output of coacervate dissolution. Such dynamical phase separations could pave the way to controllable functions within synthetic cells.

4.2.2. Reaction Centers

The ability of coacervates to accelerate enzyme reactions has been readily transposed to encapsulated coacervate droplets. As discussed in Section 3, Beneyton et al. reported the catalytic activity of formate dehydrogenase within single CM-dex/PDDA and pLys/ATP complex coacervates encapsulated within water-in-oil microfluidic emulsion droplets.[154] Several other studies have reported single enzyme[170,216,217,223] or two-enzyme cascade[220] reactions, as well as cell-free DNA transcription,[160,215] in organelle-like coacervates encapsulated in different types of compartments, including water-in-oil emulsion droplets,[160] lipid-based giant

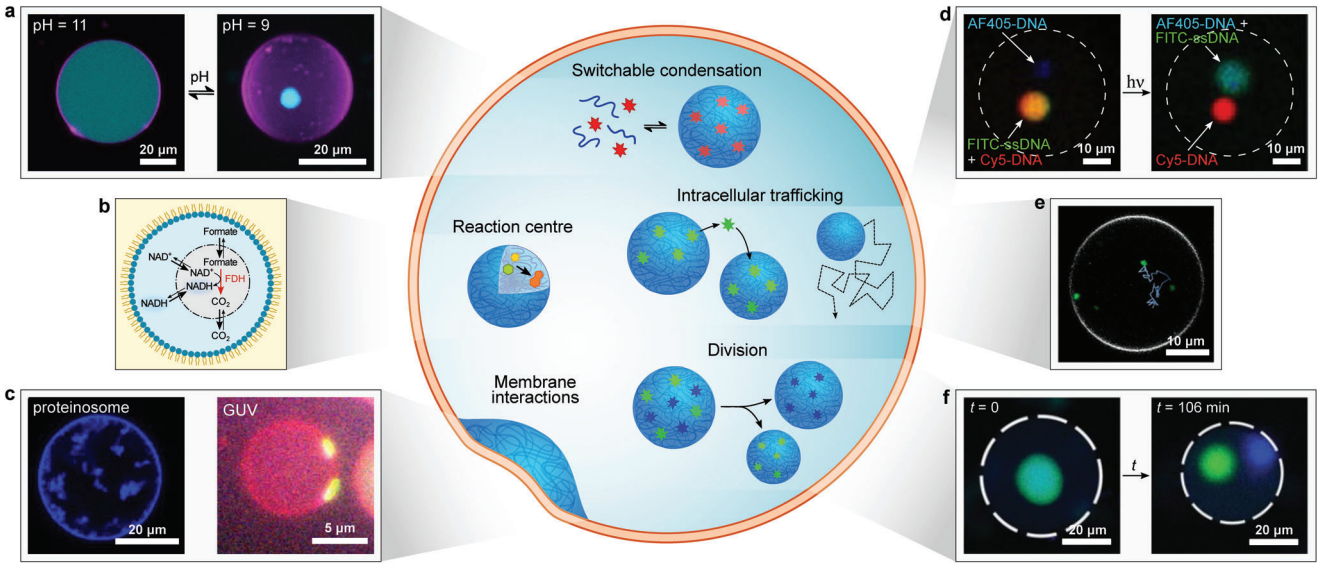

Figure 7. Functions of organelle-like coacervates encapsulated within membrane-bounded compartments. a) pH-mediated reversible coacervation of pLys and ATP within GUVs. Reproduced under the terms of the CC-BY license.[217] Copyright 2020, The Authors. Published by Wiley-VCH. b) Conversion of formate into CO_2 by formate dehydrogenase (FDH) in the presence of NAD^+ cofactor in pLys/ATP coacervates encapsulated in w/o emulsion droplets. Reproduced with permission.[154] Copyright 2020, Wiley-VCH. c) Adhesion of encapsulated PDDA/chlorhexidine (CHDX) coacervates (left) and cholesterol-functionalized polyU/spermine (left) coacervates on the inner side of proteinosomes and GUVs, respectively. Left: Reproduced under the terms of the CC-BY license.[216] Copyright 2019, The Authors. Published by Wiley-VCH. Right: Reproduced with permission.[218] Copyright 2020, American Chemical Society. d) Light-activated directional trafficking of fluorescein isothiocyanate (FITC)–ssDNA from Cy5-labeled DNA coacervates to AF405-tagged DNA droplets encapsulated in w/o emulsion droplets. Reproduced with permission.[132] Copyright 2022, Wiley-VCH. e) Enzyme-powered motion of a terpolymer-stabilized complex coacervate inside a GUV. Reproduced under the terms of the CC-BY license.[225] Copyright 2022, The Authors. Published by American Chemical Society. f) Light-driven splitting of a single DNA coacervate into two droplets inside a GUV. Reproduced under the terms of the CC-BY license.[230] Copyright 2022, The Authors. Published by Wiley-VCH.

unilamellar vesicles,[215,217] and proteinosomes.[170,216,220] In an illustrative example, Deng and Huck spatially organized the DNA-directed synthesis of RNA aptamers via in vitro transcription tools inside polyU/spermine coacervates encapsulated within liposomes.[215]

Notably, dynamical coacervation has started being exploited to control enzyme reactions within membrane-bounded compartments. The pH-driven formation of pLys/ATP coacervates within GUVs was shown to activate a formate dehydrogenase reaction due to the local enzyme upconcentration.[217] This study exemplifies the potential of encapsulated coacervates as organelle-like modules to dynamically regulate biochemical reactions in synthetic cells. Combined with more programmable biomolecular recruitment strategies, dynamical coacervation could be used as a robust approach to coordinate multiple reactions in space and time within the confined interior of a synthetic cell. Notably, the selective upconcentration of one enzyme upon coacervate formation could be used to redirect metabolic fluxes in a branched pathway involving two enzymes, as reported in cellulo using light-switchable condensates.[71]

4.2.3. Localization at Membranes and Membrane Remodeling

Coacervates encapsulated within compartments can interact with the inner side of the membrane. In an example, Booth et al. have taken advantage of coacervate/membrane interactions to control the spatial positioning of coacervates by reversible trapping at the inner surface of proteinosomes.[216] In their study, negatively charged chlorhexidine/CM-dex complex coacervates were reported to nucleate and form within proteinosomes, whose protein shell also exhibited a negative surface potential, while slightly positively charged PDDA/ATP droplets were attracted to the inner surface of to form a thin submembrane layer (Figure 7c). Increasing the ionic strength weakened the attractive electrostatic interaction with the proteinosome membrane, which reshapes the coacervate sublayer into dispersed droplets within the proteinosome lumen.[216]

Moving toward more biologically relevant membranes, Last et al. investigated adhesive interactions between GUV-forming lipid bilayers and encapsulated coacervates.[218] They observed that pLys/ATP coacervates tended to stick to and move along the inner leaflet of the membrane instead of randomly diffusing within the GUVs, which was attributed to electrostatic attraction between the positively charged droplets and oppositely charged lipids added into the membrane. Coacervates assembled from cholesterol-functionalized polyU and pLys developed even stronger attractive interactions with the membrane (Figure 7c), which was attributed to the anchoring of cholesterol into the hydrophobic bilayer environment.[218] This stronger adhesion further resulted in wetting of the membrane by coacervate droplets, which impacted the local lipid-membrane structure due to elastocapillary forces similar to those generated by condensates on membranes in living cells.[186]

Knowledge gained from fundamental studies on capillary forces generated by coacervates on membranes (see Section 3)

Table 1. Functions of organelle-like coacervate droplets encapsulated within membrane-bounded compartments.

Organelle function	Compartment	Coacervate system[a)]	Reference
n/d[b)]	w/o emulsion	pLys/ATP, PDDA/ATP	[154]
		DEAD-box ATPase Dhh1/RNA	[213]
		FUS, FUS/polyU	[214]
	GUV	pLys/ATP pArg/CoA	[215]
	Proteinosome	CHXD/CM-dex	[216]
Switchable condensation	w/o emulsion	Peptide/PSS, peptide/polyU (chemical reaction)	[212]
		ELP (temperature)	[194,221–223]
		RGG-based IDP (light) (enzyme reaction)	[173,181]
	GUV	Spermine/polyU (temperature) (enzyme reaction)	[215,178]
		pLys/ATP (pH)	[178,217,218]
		pLys/CM-dex (pH)	[217]
	Proteinosome	DEAE-dex/*trans*-AzoGlu2 (light, enzyme reaction)	[170]
	Polymersome	PAH/ATP (pH, enzyme reaction)	[219]
	Colloidosome	pLys/ATP (pH, temperature)	[226]
Reaction center	w/o emulsion	pLys/CM-dex, PDDA/CM-dex	[154]
		ELP (in partially dewetted w/o emulsion)	[223]
	GUV	Spermine/polyU	[215]
		pLys/ATP	[217]
	Proteinosome	PDDA/ATP	[216]
		PDDA/Su-dex	[220]
		DEAE-dex/*trans*-AzoGlu2	[170]
Membrane interactions	GUV	pLys/ATP Spermine/polyU	[218]
	Proteinosome	PDDA/ATP	[216]
Intracellular trafficking	w/o emulsion	DNA nanostars	[132]
	GUV	Q-Am/CM-Am	[225]
Division	w/o emulsion, GUV	DNA nanostars	[230]

[a)] pLys: poly-L-Lysine, ATP: adenosine triphosphate, PDDA: poly(diallyldimethylammonium chloride), RNA: ribonucleic acid, FUS: fused in sarcoma, polyU: poly(uridylic acid), pArg: poly-L-Arginine, CoA: coenzyme A, CHXD: chlorhexidine, CM-dex: carboxymethyl-dextran, PSS: polystyrene sulfonate, ELP: elastin-like polypeptide, IDP: intrinsically disordered protein, DEAE-dex: diethylaminoethyl dextran, *trans*-AzoGlu2: *trans*-azobenzene diglutamate, PAH: poly(allylamine hydrochloride), Su-dex: succinylated dextran, DNA: deoxyribonucleic acid, Q-Am: quaternized amylose, CM-Am: carboxymethyl-amylose; [b)] n/d: no determined function.

could be applied to encapsulated coacervates to control more dynamically their interactions with the inner leaflet of lipid bilayers. Possible outcomes of such programmable coacervate–membrane interactions could be the local recruitment of proteins at the membrane, the remodeling of membranes, e.g., to achieve internally triggered endocytosis, or the alteration of the membrane permeability (e.g., via a change in lipid packing[205]), which could ultimately regulate signal transduction across membranes.

4.2.4. Intracellular Trafficking

Chemical Trafficking between Organelles: Living cells rely on complex biochemical processes and machineries to ensure that given molecules are addressed to specific organelles. Such a precise intracellular trafficking is crucial to the orchestration and synchronization of multiple reactions. Inspired by the multicompartmentalized architecture of modern cells, the integration of different specialized organelles within synthetic cells would provide an integrated approach to perform different functions by selectively addressing signaling molecules to specific locations. Promisingly, Zhao et al. recently reported the formation of physically separated (immiscible) two or three DNA nanostar coacervates within water-in-oil microfluidic droplets.[132] Using this platform, light-driven bidirectional trafficking of single-stranded DNA molecules from one coacervate to the other was demonstrated (Figure 7d). This process was driven by unfolding of azobenzene-functionalized hairpin sticky ends in the DNA droplets upon light-activated *trans–cis* azobenzene photoisomerization, resulting in changes in the base pairing affinity of the ssDNA with the droplets, therefore triggering their migration from one coacervate to the other.

Other approaches toward selective and switchable partitioning (discussed in Section 3) could also be implemented to trigger selective release or capture of biomolecules from organelle-like coacervates. The integration of more than two coacervates would also allow to coordinate multiple reactions in networked organelle-like coacervates, and thus establish signaling

cascades for the sequential processing of molecules reminiscent to metabolic routes in living cells. Integrating both coacervate-based and membrane-bounded organelles could also offer more versatility in the selective addressability and processing of molecules in synthetic cells. There is of course still a long way to reach such a level of complexity, but these developments will certainly benefit from a deeper understanding of chemical communication pathways in populations of coacervate droplets.[115,227,228]

Organelle Transport: A more intricate approach toward intracellular trafficking in synthetic cells would involve the motion of coacervate organelles themselves (rather than relying on the diffusion of individual molecules). As a first step in this direction, Song et al. recently developed motile coacervates within lipid-based GUVs.[225] In their work, coacervates were coated with an enzyme-functionalized terpolymer membrane (see Section 5) that powered their self-diffusiophoretic motion upon addition of the enzyme substrate as chemical fuel. Due to the liquid-like nature of these membranized coacervates, the enzymes transiently clustered into asymmetric patches on the surface of the droplets, resulting in stochastic dynamics of coacervate motion (Figure 7e). In addition, the confinement of coacervates within GUVs was reported to hinder their motion, which led to a subdiffusive regime, although normal diffusion could be restored by addition of more fuel.[225]

Coacervate motion within the confined interior of microcompartments could be exploited in future studies to transport functional molecules over long distances in synthetic cells. These developments would yet require a finer control over coacervate displacement to achieve directional transport. A possible strategy toward this goal could be to take inspiration from living cells, where energy-fueled kinesin motor proteins ensure the directional transport of cargo vesicles along microtubules. Interestingly, such a process was recently reported for the transport of small unilamellar vesicles along artificial DNA cytoskeleton fibers within GUVs, based on ATP-triggered DNA polymerization.[229]

4.2.5. Organelle Division

Achieving synthetic cell division is another important milestone that has attracted strong attention. A challenging task is achieving symmetric division, where the contents of synthetic cells would be split evenly in the second-generation compartments. Taking the example of DNA segregation, living cells utilize complex nanomachineries, the eukaryotic mitotic spindle, or the bacterial Par system, to distribute evenly the genetic material during cell division. The controllable division of coacervate droplets could provide a simple strategy to achieve DNA segregation during synthetic cell division. Remarkably, by rationally designing DNA–RNA chimera strands, Sato et al. have recently reported the fission of DNA nanostar coacervate droplets using ribonuclease A to degrade the linking RNA parts, leading to splitting of two kinds of three-armed nanostars (called Y-motifs).[66] Due to their intrinsic orthogonality, these Y-motifs could not mix in the absence of the RNA linking part, which gradually resulted in the separation of a single DNA coacervate into two droplets composed of the two different Y-motifs. In addition, Tran et al. also developed a light-cleavable linker between two kinds of Y-motifs, which allowed spatiotemporal control over the DNA coacervate fission process.[230] Strikingly, using this approach, DNA segregation via coacervate fission was recently demonstrated inside cell-sized compartments, including water-in-oil droplets and GUVs[230] (Figure 7f).

While such a DNA segregation module offers a promising strategy to control the segregation of DNA, many steps still need to be taken to achieve concerted division of the membrane-bounded compartment and coacervate fission. In addition, it is still unclear how to ensure that the divided coacervates distribute evenly in the second-generation compartments to achieve a true symmetric division. Perhaps interactions between coacervates and the membrane (possibly coupled to membrane remodeling, see above) or the incorporation of a dynamic cytoskeleton could help in the spatial positioning of coacervates during division.[231] Last, synthetic cell division would be incomplete without a preliminary growth mechanism that ensures duplication of the internal material content and increase in the surface area of the to-be-divided compartment. Active coacervate growth processes identified in Section 3, e.g., via the synthesis (or, ultimately, the self-replication) of DNA, could provide a possible solution.

5. Coacervates as Cytosol-Like Templates for Synthetic Cells

In their pioneering studies, Bungenberg de Jong and Kruyt evoked the resemblance of coacervates with the crowded interior of cells.[2] Compellingly, several studies have started exploring this potential and used coacervates to direct the assembly of a membrane, host organelle-like subcompartments, and localize a cytoskeleton (**Table 2** and **Figure 8**). In this section, we illustrate these different directions that make coacervate droplets a step closer to cytosol-like templates for the construction of integrated synthetic cells.

5.1. Interfacial Membrane Self-Assembly

5.1.1. Of the Thermodynamic Instability of Coacervate Droplets

Coacervate microdroplets are thermodynamically unstable and coarsen overtime to ultimately macroscopically phase separate into a bulk coacervate phase and a dilute supernatant. Based on optical microscopy observations, and despite a lack of quantitative experimental studies, the coarsening of coacervate has been attributed to Brownian-motion-induced coalescence events combined with gravity-driven sedimentation (for polymer- or DNA-based coacervates) or creaming (for some surfactant systems that are less dense than water). For its part, Ostwald ripening has been shown not to occur for pLys/ATP complex coacervates,[176] which was attributed to the high energy or interfacial entropy barrier associated to the transfer of pLys or neutral pLys/ATP complexes from one droplet to the other via the continuous phase.

Different strategies have been explored to stabilize complex coacervates, including electrostatic repulsion – by altering the positive to negative molar charge ratio (and hence the excess surface charge on the droplets) – or, more intriguingly, dispersion of the bulk coacervate phase (collected after centrifugation) into

Table 2. Template roles of coacervate droplets for synthetic cell assembly.

Template property	Nature	Coacervate system[a)]	Reference
Interfacial membrane assembly	Fatty acids	PDDA/ATP, pLys/ATP, pLys/RNA	[244]
		pLys/DNA	[245]
	Phospholipids	Protamine sulfate, PDDA/PAA	[246]
		DEAE-dex/DNA	[247]
		PRM-based IDP	[248]
		PDDA/DNA	[249]
		PEAD/heparin	[250]
	Surfactants	pLys/DNA	[251]
		PEI/DNA	[252]
	Oligopeptides	PAH/pGlu	[148]
	Polyelectrolytes	PDDA/PAA	[254]
	Protein–polymer conjugates	Q-Am/Su-Am	[253]
	Block copolymers	Q-Am/CM-Am	[129,255–258]
	Small unilamellar vesicles	Spermine/polyU	[165]
		PDDA/PAA, PAH/PAA, PAH/ADP	[235]
		PDDA/ATP, PDDA/PAA, PEI/ATP	[236]
	Nanoparticles	PDDA/ATP, PDDA/PAA	[237]
		PDDA/CM-dex	[238]
		Q-Am/CM-Am	[239]
	Microgels	Polyampholyte	[240]
	Cell fragments	Q-Am/HA	[241]
		DEAE-dex/DNA	[242]
	Bacteria	PDDA/ATP	[243]
Organelle confinement	Proteinosome	Fatty acids	[150]
	Polymersome	Q-Am/CM-dex	[256]
	Colloidosome	PDDA/CM-dex	[238]
	Chloroplast	Q-Am/HA	[241]
		PDDA/CM-dex	[265]
	Bacteria	Q-Am/HA	[241]
		PDDA/ATP	[243]
Cytoskeleton self-assembly	FtsZ	pLys/RNA	[202]
		pLys/GTP	[203]
	Actin	pLys/pGlu	[137]
		FUS	[200]
	DNA nanotube	PDDA/PAA	[149]

[a)] See legend of Table 1, PEI: polyethyleneimine, HA: sodium hyaluronate, PEAD: poly(ethylene argininylaspartate diglyceride), Su-Am: succinyl amylose, pGlu: poly-L-glutamic acid, GTP: guanosine triphosphate.

deionized water.[232,233] While the former case may appear as a general phenomenon to complex coacervate systems, the latter is likely highly system-dependent, and has only been reported for PDDA/ATP coacervates produced either via microfluidics[232] or in bulk.[233] Stabilization was attributed to the ejection of counterions localized to the droplet surface into the continuous ion-free water after coacervate redispersion, which was suggested to strengthen PDDA/ATP interactions at the interface, presumably producing a physically cross-linked layer providing steric repulsions between droplets.[233] In the following section, we will see that the intrinsic thermodynamic instability of coacervate droplets has also motivated the development of alternative stabilization approaches based on interfacial membrane self-assembly.

5.1.2. Coacervate-Guided Membrane Self-Assembly

Membranization has appeared in the past few years as a promising strategy to enhance the stability of coacervates against fusion and external variations, as recently reviewed.[234] Differing from the encapsulation of organelle-like coacervates within membrane-bounded compartments, membranization involves the self-assembly of (macro)molecules or particles at the surface of coacervates to produce a semipermeable shell. From this viewpoint, coacervate droplets can be described as a cytosol-like template that directs the assembly of a membrane-like envelope. A broad palette of building blocks has been reported to induce membranization of coacervate droplets. Schematically, these can be divided into two main classes, namely, i)

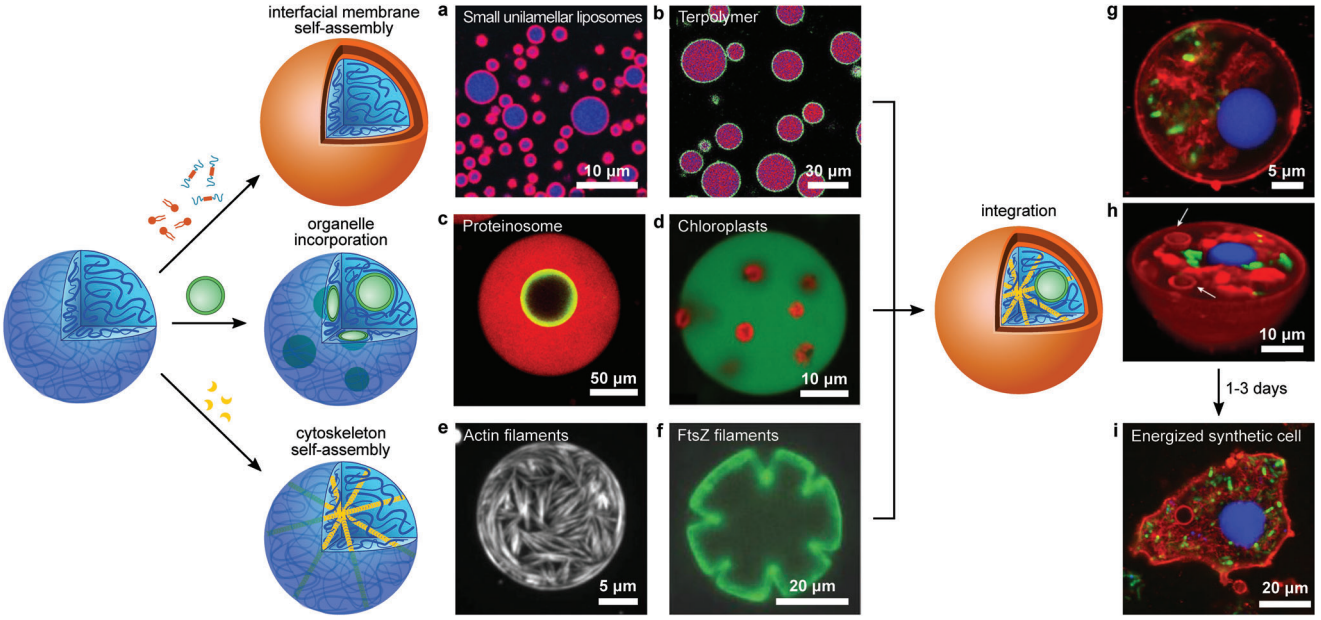

Figure 8. Coacervates as cytosol-like templates for the construction of synthetic cells. Coacervates can guide the interfacial assembly of a membrane, host organelles, and reshape upon internal cytoskeleton self-assembly. a,b) Interfacial adsorption of small unilamellar vesicles and triblock copolymers on polyU/spermine and oppositely charged amylose coacervates, respectively. a) Reproduced with permission.[165] Copyright 2016, American Chemical Society. b) Reproduced with permission.[255] Copyright 2017, American Chemical Society. c,d) Spontaneous capture of proteinosomes and chloroplasts by fatty acid and PDDA/ATP coacervates, respectively. c) Reproduced under the terms of the CC-BY license.[150] Copyright 2018, The Authors. Published by Springer Nature. d) Reproduced under the terms of the CC-BY license.[265] Copyright 2018, The Authors. Published by The Royal Society of Chemistry. e,f) Self-assembly of actin and FtsZ filaments in pLys/pGlu and pLys/GTP coacervates, respectively. e) Reproduced with permission.[137] Copyright 2018, Elsevier. f) Reproduced with permission.[203] Copyright 2018, Wiley-VCH. g–i) Integration of organelle-like live bacteria in membranized PDDA/UTP coacervates sustains long-term metabolic activity to produced energized synthetic cells that undergo morphological changes over time into a eukaryotic amoeba-like architecture. Reproduced with permission.[243] Copyright 2022, Springer Nature Limited.

nano- or microscale objects (Figure 8a), such as liposomes (small unilamellar vesicles),[165,235,236] nanoparticles,[237–239] microgels,[240] cell fragments,[241,242] or even living cells;[243] ii) amphiphilic (macro)molecules (Figure 8b), including fatty acids,[244,245] phospholipids,[246–250] surfactants,[251,252] protein–polymer conjugates,[253] self-assembling oligopeptides,[148] comb polyelectrolytes,[254] or block copolymers.[255–258]

Depending on the nature of the membrane-forming components, different mechanisms may explain their interfacial adsorption on coacervates. The adsorption energy of nano- or microscale objects, which scales as their surface area, is sufficiently high to counterbalance the low surface tension of coacervates, and stabilization is accounted for by a Pickering-like effect, as reported for water–water interfaces produced by segregative LLPS.[259] In comparison, the self-assembly of small amphiphiles into larger structures, together with differential interactions with the coacervate and supernatant phases, may account for their preferential affinity for the interface. For instance, fatty acids were shown to form a multilamellar structure around complex coacervates that was likely thick enough to fill the interface.[244] In other studies, phospholipids were shown to form a single bilayer around simple and complex coacervates.[246,247] Block terpolymers composed of a PEG-*b*-poly(caprolactone-*gradient*-trimethylene carbonate) (PCL*g*TMC)-*b*-poly(glutamic acid) (pGlu) sequence were rationally designed to stabilize amylose-based complex coacervates.[255–257] Here, the hydrophilic charged pGlu and neutral PEG blocks provided electrostatic anchoring to the coacervate phase and steric repulsion in the supernatant, respectively, while the middle PCL*g*TMC drove hydrophobic chain association. This terpolymer was assumed to have a sufficient length to span the coacervate/water interface.[257] Last, components forming a "gelled" corona, e.g., via polymer cross-linking[260] or gelation[261] or DNA hybridization,[196] have also been reported to prevent coacervate fusion.

Remarkably, membranization brings new functionalities to coacervate droplets, the first of which is semipermeability. Indeed, the uptake of solutes by membrane-coated coacervates does no longer rely solely on the sequestration properties (partitioning) of the coacervate phase but also on the permeability of the enclosing membrane. Nano- or microscale stabilizers typically result in shells with relatively large pores, allowing the unrestricted diffusion of both small and large molecules.[165,239] Surprisingly, lipid- and polymer-coated coacervates have been shown to retain their capacity to spontaneously accumulate small molecules and ions, such as glucose, hydrogen peroxide, or magnesium ions, but also larger macromolecules, including dextran chains, proteins, RNA, and DNA, suggesting the existence of defects/pores in the membrane.[246,247,257] These defects/pores can be viewed as either detrimental (as they allow unrestricted diffusion of both small and large solutes) or advantageous (since they facilitate solute exchange with the environment) depending on the considered function. For instance, DNA-[133] and protein-based[262] signaling molecules could be transported

between different terpolymer-membrane-bounded coacervates to achieve signal communication in synthetic cell populations.

Several questions about the organization of lipids at coacervate/supernatant, and more generally water–water, interfaces remain. In particular, the lipid organization may be perturbed by the high charge densities and peculiar interfacial properties of coacervates. For instance, in a study, charge and polar interactions between phospholipids present in the inner membrane leaflet and polyelectrolytes at the surface of coacervates were shown to improve the robustness and reduce the fluidity of the membrane compared to water-filled GUVs.[247] Other simple systems lacking long-range electrostatic interactions, such as segregative PEG/dextran LLPS, could help in elucidating the critical parameters governing the self-assembly behavior of lipids at water–water interfaces.[263]

On a last note, enzyme activity has also been embedded in coacervate-templated polymer membranes, which has been used to impart motility to coacervates in the presence of substrate due to the stochastic distribution of membrane-tethered enzymes.[264] This example illustrates the possibility to functionalize coacervate-enclosing membranes with enzymes, possibly paving the way to controllable transmembrane signal transduction.

5.2. Incorporation of Organelle-Like Subcompartments

Beyond membranization, coacervate droplets have been shown to be able to host different types of subcompartments, providing a first step toward coacervate-based multicompartmentalized synthetic cells. The coexistence of multiple coacervate phases (see Section 3) can be viewed as a simple approach to achieve hierarchical organization:[187–189] in this case, the outer coacervate phase is described as the cytosol-like medium, while the inner coacervate is viewed as a membraneless organelle. Such coacervate-in-coacervate multicompartmentalized synthetic cells have been used for the spatial organization of cascade enzyme reactions.[191]

Excitingly, coacervate droplets also accommodate membrane-bounded organelles. In an example, proteinosomes were shown to be spontaneously captured by fatty acid micelle coacervates via electrostatically mediated wetting to produce nested organelles within a cytosol-like dense phase capable of enzyme-based chemical coupling (Figure 8c).[150] Other studies reported the incorporation of either synthetic or biological compartments within coacervate microdroplets. As an example, Mason et al. produced a polymersome-in-coacervate system, where both activation of cascade processes and segregation of incompatible enzymes were achieved.[256] Recently, Gao et al. developed gold-nanoparticle-coated coacervate droplets whose membrane was able to be unlocked by ligand dissociation under light irradiation or chemical cleavage to achieve triggerable capture of organelle-like colloidosomes into coacervate interior.[238] In other studies, chloroplasts extracted from spinach leaves were sequestered within complex coacervates based on attractive electrostatic interactions (Figure 8d), and shown to retain their intact structure and photosynthetic activity.[241,265] Last, the confinement of organelle-like living bacteria within coacervates has also recently been reported.[241,243] Summarizing these studies, the driving force of compartment capture by coacervates appears to be a combination of attractive interactions and wetting.

5.3. Shaping via Cytoskeleton Self-Assembly

The analogy between coacervates and the cell cytosol would be incomplete without the demonstration of cytoskeleton self-assembly and associated coacervate deformations. The cellular cytoskeleton is a dynamic network of protein filaments present in the cytoplasm, which plays a key role for cell mechanics, primarily shaping cells and providing them mechanical resistance against external forces. Recent works have started investigating the interactions between coacervates and cytoskeletal proteins,[231] such as actin[137,200] (Figure 8e) and FtsZ.[202,203] Shape deformations into elongated[200] or flower-like[203] coacervates (Figure 8f) have been observed as a result of filament sequestration or localized self-assembly. Remarkably, the self-assembly of FtsZ monomers into dynamic filaments in the presence of high concentrations of guanosine triphosphate (GTP) within pLys/RNA complex coacervates resulted in the elongation of the droplets along the fibrils until their division into two.[202] Inspired by the role of biomolecular condensate in the nucleation of microtubules by concentrating tubulin in living cells,[266] coacervate droplets could be used to trigger the self-assembly of natural or artificial cytoskeleton filaments and position them in synthetic cells to achieve morphological changes of the membrane-bound compartment itself.

5.4. Integration: Toward Coacervate-Based Self-Sustained Synthetic Cells

A grand challenge in the bottom-up construction of synthetic cells is the integration of different structural and functional features within a single compartment. Based on their cytosol-like properties evidenced above, coacervate droplets offer a possible approach toward this goal (Figure 8g–i). Interestingly, a few studies have already demonstrated the integration of organelle-like subcompartments within membrane-coated coacervates. In an example, enzyme-loaded polymersomes played the role of catalytically active organelles within terpolymer-stabilized complex coacervates, and ensured the spatial segregation of different enzymes involved in a cascade reaction.[256] In another study, chloroplast or even live bacteria were used as functional organelles within complex coacervates stabilized by bacterial fragments.[241]

The most integrated coacervate-templated synthetic cells have been reported recently by Xu et al.[243] In this work, PDDA/ATP complex coacervates were first shown to spatially position two bacteria strains at different locations: as demonstrated by confocal fluorescence microscopy imaging coupled to statistical fluorescence activated cell sorting (FACS) screening, live *Escherichia coli* (*E. Coli*) bacteria were spontaneously captured within the droplets while *Pseudomonas aeruginosa* adsorbed at the coacervates interface. Biochemical lysis of the bacteria resulted in the release of their biological contents within the coacervate matrix and the formation of a semipermeable shell around the droplets

with lipid bilayers fragments. Bacterial enzymes entrapped in the as-formed membranized coacervate droplets remained active and, the bacterial DNA could be fragmented and condensed using histone and CM-dex into a DNA-rich, nucleus-like structure. ATP-fueled actin polymerization was also demonstrated within the constructs. Remarkably, live *E. coli* was also implanted into the coacervate droplets to act as mitochondria surrogates and produce chemical energy in the form of ATP over long periods of time. Strikingly, this energization resulted in morphological changes of the spherical coacervate droplets into amoeba-like shapes, which was attributed to the prolonged metabolic activity of entrapped bacteria that altered the interfacial properties of the coacervates.

This example illustrates the potential of interfacing living cells with coacervates to build self-sustained compartments. In order to build fully synthetic cells without relying on living systems, future studies will need to explore alternative design strategies to integrate artificial metabolic modules able to produce energy when coupled to an external source of energy (such as light or nutrients).[267]

6. Conclusion and Outlook

In conclusion, the peculiar properties of coacervates offer exciting avenues for the bottom-up assembly of synthetic cells. Their role as organelle-like modules or cytosol-like chassis has started being explored in several illustrative studies, showcasing the potential of these chemically rich, crowded droplets in supporting various bioinspired functions under confined conditions. By harnessing the power of biomimicry, studying liquid–liquid phase separation in synthetic cells offers unprecedented opportunities to investigate in well controlled environments processes occurring in living cells, such as the dynamical behaviors and functions of biomolecular condensates. In the longer run, building integrated synthetic cells that capitalize on the peculiar properties of coacervate microdroplets could offer new perspectives for applications in therapeutics or environmental cleanup. Achieving scalability and programmability of coacervates in synthetic cells appears as a crucial step for their successful integration into applications.

Several challenges still need to be tackled to develop fully integrated synthetic cells. From the organelle-like perspective, the precise positioning of coacervate droplets within compartments remains to be demonstrated. Using different coacervate droplets to direct metabolic fluxes and coordinate signaling cascades will also require to develop new tools to precisely direct molecules from one coacervate droplet to another, e.g., using selective sequestration or reversible coacervate formation. It is also still unclear how to achieve coordinated growth and division of both coacervate organelles and the enclosing compartment to perform symmetric division. From a cytosol-like template viewpoint, achieving both catabolic and anabolic reactions in the same compartment will require to be able to confine incompatible enzyme reactions in different locations. Ultimately, powering these coacervate-based synthetic cells will necessitate to couple the internal processes to an external source of energy, e.g., light or chemical nutrients.

Acknowledgements

Z.L. acknowledges funding from the Chinese Scholarship Council. J.-C.B. acknowledges the support by the "Fondation Simone et Cino Del Duca," the "Agence Nationale de la Recherche" (Grant No. ANR-20-CE06-0011), and the Université de Bordeaux Research Network Frontiers of Life. N.M. acknowledges funding from the IdEx Bordeaux (Grant No. ANR-10-IDEX-03-02), an "Investissement d'Avenir" program of the French government managed by the "Agence Nationale de la Recherche," the "Région Nouvelle-Aquitaine" (Grant No. AAPR 2020-2019-8330510), and the "Agence Nationale de la Recherche" (Grant No. ANR-21-CE06-0022).

Conflict of Interest

The authors declare no conflict of interest.

Keywords

biomolecular condensates, coacervates, liquid–liquid phase separation, membraneless organelles, synthetic cells

Received: April 14, 2023
Revised: June 15, 2023
Published online:

[1] F. W. Tieback, *Z. Chem. Ind. Kolloide* **1911**, *8*, 198.
[2] H. G. Bungenberg de Jong, H. R. Kruyt, *Proc. K. Ned. Akad. Wet.* **1929**, *32*, 849.
[3] A. I. Oparin, *The Origin of Life*, Dover Publications, New York **1938**.
[4] T. H. Kalantar, C. J. Tucker, A. S. Zalusky, T. A. Boomgaard, B. E. Wilson, M. Ladika, S. L. Jordan, W. K. Li, X. Zhang, C. G. Gosh, *J. Cosmet. Sci.* **2007**, *58*, 375.
[5] A. Madene, M. Jacquot, J. Scher, S. Desobry, *Int. J. Food Sci. Technol.* **2006**, *41*, 1.
[6] R. J. Stewart, C. S. Wang, I. T. Song, J. P. Jones, *Adv. Colloid Interface Sci.* **2017**, *239*, 88.
[7] J. T. G. Overbeek, M. J. Voorn, *J. Cell. Comp. Physiol.* **1957**, *49*, 7.
[8] I. Michaeli, J. T. G. Overbeek, M. J. Voorn, *J. Polym. Sci.* **1957**, *23*, 443.
[9] N. Martin, *ChemBioChem* **2019**, *20*, 2553.
[10] C. P. Brangwynne, C. R. Eckmann, D. S. Courson, A. Rybarska, C. Hoege, J. Gharakhani, F. Jülicher, A. A. Hyman, *Science* **2009**, *324*, 1729.
[11] C. P. Brangwynne, P. Tompa, R. V. Pappu, *Nat. Phys.* **2015**, *11*, 899.
[12] C. D. Keating, N. Martin, M. M. Santore, *Curr. Opin. Colloid Interface Sci.* **2021**, *56*, 101527.
[13] N. A. Yewdall, A. A. M. André, T. Liu, E. Spruijt, *Curr. Opin. Colloid Interface Sci.* **2021**, *52*, 101416.
[14] S. Koga, D. S. Williams, A. W. Perriman, S. Mann, *Nat. Chem.* **2011**, *9*, 720.
[15] F. Pir Cakmak, S. Choi, M. O. Meyer, P. C. Bevilacqua, C. D. Keating, *Nat. Commun.* **2020**, *11*, 5949.
[16] D. Garenne, L. Béven, L. Navailles, F. Nallet, E. J. Dufourc, J.-P. Douliez, *Angew. Chem., Int. Ed.* **2016**, *55*, 13475.
[17] M. Abbas, W. P. Lipinski, K. K. Nakashima, W. T. S. Huck, E. Spruit, *Nat. Chem.* **2021**, *13*, 1046.
[18] B. Ghosh, R. Bose, T.-Y. D. Tang, *Curr. Opin. Colloid Interface Sci.* **2021**, *52*, 101415.
[19] N. Martin, J.-P. Douliez, *ChemSystemsChem* **2021**, *3*, 2100024.
[20] P. A. Albertsson, in *Partition of Cell Particles and Macromolecules*, 3rd ed., Wiley-Interscience, New York **1986**.

[21] K. Bergfeldt, L. Picullel, P. Linse, *J. Phys. Chem.* **1996**, *100*, 3680.
[22] P. J. Flory, in *Principles of Polymer Chemistry*, 13th ed., Cornell University Press, Ithaca, NY **1953**.
[23] C. E. Sing, *Adv. Colloid Interface Sci.* **2017**, *239*, 2.
[24] C. E. Sing, S. L. Perry, *Soft Matter* **2020**, *16*, 2885.
[25] J. J. Madinya, C. E. Sing, *Macromolecules* **2022**, *55*, 2358.
[26] M. S. Long, C. D. Jones, M. R. Helfrich, L. K. Mangeney-Savin, C. D. Keating, *Proc. Natl. Acad. Sci. USA* **2005**, *102*, 5920.
[27] C. D. Keating, *Acc. Chem. Res.* **2012**, *45*, 2114.
[28] S. R. MacEwan, A. Chilkoti, *Pept. Sci.* **2010**, *94*, 60.
[29] N. K. Li, F. G. Quiroz, C. K. Hall, A. Chilkoti, Y. G. Yingling, *Biomacromolecules* **2014**, *15*, 3522.
[30] R. Merindol, S. Loescher, A. Samanta, A. Walther, *Nat. Nanotechnol.* **2018**, *13*, 730.
[31] W. Liu, A. Samanta, J. Deng, C. O. Akintayo, A. Walther, *Angew. Chem., Int. Ed.* **2022**, *61*, e202208951.
[32] R. Merindol, N. Martin, T. Beneyton, J. C. Baret, S. Ravaine, *Adv. Funct. Mater.* **2021**, *31*, 2010396.
[33] J. Dinic, A. B. Marciel, M. V. Tirrell, *Curr. Opin. Colloid Interface Sci.* **2021**, *54*, 101457.
[34] A. Perro, L. Giraud, N. Coudon, S. Shanmugathasan, V. Lapeyre, B. Goudeau, J.-P. Douliez, V. Ravaine, *J. Colloid Interface Sci.* **2019**, *548*, 275.
[35] M. Rubinstein, A. V. Dobrynin, *Trends Polym. Sci.* **1997**, *5*, 181.
[36] M. A. Winnik, A. Yekta, *Curr. Opin. Colloid Interface Sci.* **1997**, *2*, 424.
[37] J. van der Gucht, E. Spruijt, M. Lemmers, M. A. Cohen Stuart, *J. Colloid Interface Sci.* **2011**, *361*, 407.
[38] D. Priftis, N. Laugel, M. Tirrell, *Langmuir* **2012**, *28*, 15947.
[39] X. Liu, J.-P. Chapel, C. Schatz, *Adv. Colloid Interface Sci.* **2017**, *239*, 178.
[40] I. B. A. Smokers, M. H. I. van Haren, T. Lu, E. Spruijt, *ChemSystemsChem* **2022**, *4*, 202200004.
[41] J. Wang, M. Abbas, J. Wang, E. Spruijt, *ChemRxiv* **2021**, https://doi.org/10.26434/chemrxiv-2021-1zt9k.
[42] C. L. Cooper, P. L. Dubin, A. B. Kayitmazer, S. Turksen, *Curr. Opin. Colloid Interface Sci.* **2005**, *10*, 52.
[43] E. Kizilay, A. B. Kayitmazer, P. L. Dubin, *Adv. Colloid Interface Sci.* **2011**, *167*, 24.
[44] T. Croguennec, G. M. Tavares, S. Bouhallab, *Adv. Colloid Interface Sci.* **2017**, *239*, 115.
[45] F. Comert, P. L. Dubin, *Adv. Colloid Interface Sci.* **2017**, *239*, 213.
[46] H. Karoui, M. J. Seck, N. Martin, *Chem. Sci.* **2021**, *12*, 2794.
[47] Y. Xu, M. Mazzawi, K. Chen, L. Sun, P. L. Dubin, *Biomacromolecules* **2011**, *12*, 1512.
[48] R. A. Kapelner, A. C. Obermeyer, *Chem. Sci.* **2019**, *10*, 2700.
[49] A. C. Obermeyer, C. E. Mills, X.-H. Dong, R. J. Flores, B. D. Olsen, *Soft Matter* **2016**, *12*, 3570.
[50] C. S. Cummings, A. C. Obermeyer, *Biochemistry* **2018**, *57*, 314.
[51] Y. Li, P. L. Dubin, H. A. Havel, S. L. Edwards, H. Dautzenberg, *Langmuir* **1995**, *11*, 2486.
[52] Y. Wang, K. Komura, P. L. Dubin, *Macromolecules* **2000**, *33*, 3324.
[53] M. Wang, Y. Wang, *Soft Matter* **2014**, *10*, 7909.
[54] W. Zhao, Y. Wang, *Adv. Colloid Interface Sci.* **2017**, *239*, 199.
[55] D. Garenne, L. Navailles, F. Nallet, A. Grélard, E. J. Dufourc, J.-P. Douliez, *J. Colloid Interface Sci.* **2016**, *468*, 95.
[56] J.-P. Douliez, N. Martin, C. Gaillard, T. Beneyton, J.-C. Baret, S. Mann, L. Béven, *Angew. Chem., Int. Ed.* **2017**, *56*, 13689.
[57] F. M. Menger, B. M. Sykes, *Langmuir* **1998**, *14*, 4131.
[58] A. Bhattacharya, H. Niederholtmeyer, K. A. Podolsky, R. Bhattacharya, J.-J. Song, R. J. Brea, C.-H. Tsai, S. K. Sinha, N. K. Devaraj, *Proc. Natl. Acad. Sci. USA* **2020**, *117*, 18206.
[59] Y. Li, Y. D. Tseng, S. Y. Kwon, L. d'Espaux, J. S. Bunch, P. L. McEuen, D. Luo, *Nat. Mater.* **2004**, *3*, 38.
[60] S. Biffi, R. Cerbino, F. Bomboi, E. M. Paraboschi, R. Asselta, F. Sciortino, T. Bellini, *Proc. Natl. Acad. Sci. USA* **2013**, *110*, 15633.
[61] B. J. Jeon, D. T. Nguyen, G. R. Abraham, N. Conrad, D. F. Fygenson, O. A. Saleh, *Soft Matter* **2018**, *14*, 7009.
[62] L. Rovigatti, F. Smallenburg, F. Romano, F. Sciortino, *ACS Nano* **2014**, *8*, 3567.
[63] D. T. Nguyen, O. A. Saleh, *Soft Matter* **2017**, *13*, 5421.
[64] N. Conrad, T. Kennedy, D. K. Fygenson, O. A. Saleh, *Proc. Natl. Acad. Sci. USA* **2019**, *116*, 7238.
[65] B. J. Jeon, D. T. Nguyen, O. A. Saleh, *J. Phys. Chem. B* **2020**, *124*, 8888.
[66] Y. Sato, T. Sakamoto, M. Takinoue, *Sci. Adv.* **2020**, *6*, eaba3471.
[67] S. Do, C. Lee, T. Lee, D. N. Kim, Y. Shin, *Sci. Adv.* **2022**, *8*, eabj1771.
[68] Y. Sato, M. Takinoue, *Nanoscale Adv.* **2023**, *5*, 1919.
[69] H. Udono, J. Gong, Y. Sato, M. Takinoue, *Adv. Biol.* **2023**, *7*, 2200180.
[70] Y. Shin, J. Berry, N. Pannucci, M. P. Haataja, J. E. Toettcher, C. P. Brangwynne, *Cell* **2017**, *168*, 159.
[71] E. M. Zhao, N. Suek, M. Z. Wilson, E. Dine, N. L. Pannucci, Z. Gitai, J. L. Avalos, J. E. Toettcher, *Nat. Chem. Biol.* **2019**, *15*, 589.
[72] N. Schneider, F.-G. Wieland, D. Kong, A. A. M. Fischer, M. Hörner, J. Timmer, H. Fe, W. Weber, *Sci. Adv.* **2021**, *7*, eabd3568.
[73] E. Gomes, J. Shorter, *J. Biol. Chem.* **2019**, *18*, 7115.
[74] H. R. Kilgore, R. A. Young, *Nat. Chem. Biol.* **2022**, *18*, 1298.
[75] S. Elbaum-Garfinkel, Y. Kim, K. Szczepaniak, C. C. H. Chen, C. R. Eckmann, S. Myong, C. P. Brangwynne, *Proc. Natl. Acad. Sci. USA* **2015**, *112*, 7189.
[76] T. J. Nott, E. Petsalaki, P. Farber, D. Jervis, E. Fussner, A. Plochowietz, T. D. Craggs, D. P. Bazett-Jones, T. Pawson, J. D. Forman-Kay, A. J. Baldwin, *Mol. Cell* **2015**, *57*, 936.
[77] J. Wang, J.-M. Choi, A. S. Holehouse, H. O. Lee, X. Zhang, M. Jahnel, S. Maharana, R. Lemaitre, A. Pozniakovsky, D. Drechsel, I. Poser, R. V. Pappu, S. Alberti, A. A. Hyman, *Cell* **2018**, *174*, 688.
[78] A. Patel, H. O. Lee, L. Jawerth, S. Maharana, M. Jahnel, M. Y. Hein, S. Stoynov, J. Mahamid, S. Saha, T. M. Franzmann, A. Pozniakovski, I. Poser, N. Maghelli, L. A. Royer, M. Weigert, E. W. Myers, S. Grill, D. Drechsel, A. A. Hyman, S. Alberti, *Cell* **2015**, *162*, 1066.
[79] A. C. Murthy, G. L. Dignon, Y. Kan, G. H. Zerze, S. H. Parekh, J. Mittal, N. L. Fawzi, *Nat. Struct. Mol. Biol.* **2019**, *26*, 637.
[80] S. L. Perry, *Curr. Opin. Colloid Interface Sci.* **2019**, *39*, 86.
[81] S. L. Perry, C. E. Sing, *ACS Macro Lett.* **2020**, *9*, 216.
[82] I. Peran, T. Mittag, *Curr. Opin. Struct. Biol.* **2020**, *60*, 17.
[83] J.-M. Choi, A. S. Holehouse, R. V. Pappu, *Annu. Rev. Biophys.* **2020**, *49*, 107.
[84] V. H. Ryan, N. L. Fawzi, *Trends Neurosci.* **2019**, *42*, 693.
[85] J. D. Schmit, M. Feric, M. Dundr, *Trends Biochem. Sci.* **2021**, *7*, 525.
[86] J. A. Riback, L. Zhu, M. C. Ferrolino, M. Tolbert, D. M. Mitrea, D. W. Sanders, M.-T. Wei, R. W. Kriwacki, C. P. Brangwynne, *Nature* **2020**, *581*, 209.
[87] S. F. Banani, A. M. Rice, W. P. Peeples, Y. Lin, S. Jain, R. Parker, M. K. Rosen, *Cell* **2016**, *166*, 651.
[88] K. Bhandari, M. A. Cotten, J. Kim, M. K. Rosen, J. D. Schmit, *J. Phys. Chem. B* **2021**, *125*, 467.
[89] P. Li, S. Banjade, H.-C. Cheng, S. Kim, B. Chen, L. Guo, M. Llaguno, J. V. Hollingsworth, D. S. King, S. F. Banani, P. S. Russo, Q.-X. Jiang, B. T. Nixon, M. K. Rosen, *Nature* **2012**, *483*, 336.
[90] E. Spruijt, A. H. Westphal, J. W. Borst, M. A. Cohen Stuart, J. van der Gucht, *Macromolecules* **2010**, *43*, 6476.
[91] J. B. Schlenoff, M. Yang, Z. A. Digby, Q. Wang, *Macromolecules* **2019**, *52*, 9149.
[92] R. Kausik, A. Srivastava, P. A. Korevaar, G. Stucky, J. H. Waite, S. Han, *Macromolecules* **2009**, *42*, 7404.
[93] Y. Liu, H. H. Winter, S. L. Perry, *Adv. Colloid Interface Sci.* **2017**, *239*, 46.
[94] Q. Wang, J. B. Schlenoff, *Macromolecules* **2014**, *47*, 3108.

[95] Y. Liu, B. Momani, H. H. Winter, S. L. Perry, *Soft Matter* **2017**, *13*, 7332.
[96] S. L. Perry, L. Leon, K. Q. Hoffmann, M. J. Kade, D. Priftis, K. A. Black, D. Wong, R. A. Klein, C. F. Pierce, K. O. Margossian, J. K. Whitmer, J. Qin, J. J. de Pablo, M. Tirrell, *Nat. Commun.* **2015**, *6*, 6052.
[97] J. R. Vieregg, M. Lueckheide, A. B. Marciel, L. Leon, A. J. Bologna, J. R. Rivera, M. V. Tirrell, *J. Am. Chem. Soc.* **2018**, *140*, 1632.
[98] A. Shakya, J. T. King, *Biophys. J.* **2018**, *115*, 1840.
[99] J. Yang, *Curr. Opin. Colloid Interface Sci.* **2002**, *7*, 276.
[100] S. A. Rogers, M. A. Calabrese, N. J. Wagner, *Curr. Opin. Colloid Interface Sci.* **2014**, *19*, 530.
[101] J. P. Rothstein, H. Mohammadigoushki, *J. Non-Newtonian Fluid Mech.* **2020**, *285*, 104382.
[102] U. Capasso Palmiero, C. Paganini, M. R. G. Kopp, M. Linsenmeier, A. M. Küffner, P. Arosio, *Adv. Mater.* **2021**, *34*, 2104837.
[103] J. P. Brady, P. J. Farber, A. Sekhar, Y.-H. Lin, R. Huang, A. Bah, T. J. Nott, H. S. Chan, A. J. Baldwin, J. D. Forman-Kay, L. E. Kay, *Proc. Natl. Acad. Sci. USA* **2017**, *114*, E8194.
[104] D. M. Mitrea, B. Chandra, M. C. Ferrolino, E. B. Gibbs, M. Tolbert, M. R. White, R. W. Kriwacki, *J. Mol. Biol.* **2018**, *430*, 4773.
[105] Z. Wang, J. Lou, H. Zhang, *J. Biol. Chem.* **2022**, *298*, 101782.
[106] H. Wang, F. M. Kelley, D. Milovanovic, B. S. Schuster, Z. Shi, *Biophys. Rep.* **2021**, *1*, 100011.
[107] L. Jawerth, E. Fischer-Friedrich, S. Saha, J. Wang, T. Franzmann, X. Zhang, J. Sachweh, M. Ruer, M. Ijavi, S. Saha, J. Mahamid, A. A. Hyman, F. Jülicher, *Science* **2020**, *370*, 1317.
[108] M. Lisenmeier, M. Hondele, F. Grigolato, E. Secchi, K. Weis, P. Arosio, *Nat. Commun.* **2022**, *13*, 3030.
[109] Y. Jho, H. Y. Yoo, Y. Lin, S. Han, D. S. Hwang, *Adv. Colloid Interface Sci.* **2017**, *239*, 61.
[110] J. Qin, D. Priftis, R. Farina, S. L. Perry, L. Leon, J. Whitmer, K. Hoffmann, M. Tirrell, J. J. de Pablo, *ACS Macro Lett.* **2014**, *3*, 565.
[111] E. Spruijt, J. Sprakel, M. A. Cohen Stuart, J. van der Gucht, *Soft Matter* **2009**, *6*, 172.
[112] A. G. T. Pyo, Y. Zhang, N. S. Wingreen, *iScience* **2022**, *25*, 103852.
[113] M. Tsanai, P. W. J. M. Frederix, C. F. E. Schroer, P. C. T. Souza, S. J. Marrink, *Chem. Sci.* **2021**, *12*, 8521.
[114] M. Farag, S. R. Cohen, W. M. Borcherds, A. Bremer, T. Mittag, R. V. Pappu, *Nat. Commun.* **2022**, *13*, 7722.
[115] L. Tian, N. Martin, P. G. Bassindale, A. J. Patil, M. Li, A. Barnes, B. W. Drinkwater, S. Mann, *Nat. Commun.* **2016**, *7*, 13068.
[116] T. J. Welsh, G. Krainer, J. R. Espinosa, J. A. Joseph, A. Sridhar, M. Jahnel, W. E. Arter, K. L. Saar, S. Alberti, R. Collepardo-Guevara, T. P. J. Knowles, *Nano Lett.* **2022**, *22*, 612.
[117] A. A. Hyman, C. A. Weber, F. Jülicher, *Annu. Rev. Cell Dev. Biol.* **2014**, *30*, 39.
[118] E. A. Frankel, P. C. Bevilacqua, C. D. Keating, *Langmuir* **2016**, *32*, 2041.
[119] T.-Y. D. Tang, M. Antognozzi, J. A. Vicary, A. W. Perriman, S. Mann, *Soft Matter* **2013**, *9*, 7647.
[120] W. C. Blocher McTigue, S. L. Perry, *Small* **2020**, *16*, 1907671.
[121] K. K. Nakashima, M. A. Vibhute, E. Spruijt, *Front. Mol. Biosci.* **2019**, *6*, 21.
[122] M.-T. Wei, S. Elbaum-Garfinkle, A. S. Holehouse, C. C.-H. Chen, M. Feric, C. B. Arnold, R. D. Priestley, R. V. Pappu, C. P. Brangwynne, *Nat. Chem.* **2017**, *9*, 1118.
[123] L. Hubatsch, L. M. Jawerth, C. Love, J. Bauermann, T.-Y. D. Tang, S. Bo, A. A. Hyman, C. A. Weber, *Elife* **2021**, *10*, e68620.
[124] A. Shakya, J. T. King, *ACS Macro Lett.* **2018**, *7*, 1220.
[125] Y. Xu, M. Liu, M. Faisal, Y. Si, Y. Guo, *Adv. Colloid Interface Sci.* **2017**, *239*, 158.
[126] G. M. Tavares, T. Croguennec, P. Hamon, A. F. Carvalho, S. Bouhallab, *Food Hydrocolloids* **2015**, *48*, 238.
[127] J. J. van Lente, M. M. A. E. Claessens, S. Lindhoud, *Biomacromolecules* **2019**, *20*, 3696.
[128] W. C. Blocher McTigue, S. L. Perry, *Soft Matter* **2019**, *15*, 3089.
[129] W. J. Altenburg, N. A. Yewdall, D. F. M. Vervoort, M. H. M. E. van Stevendaal, A. F. Mason, J. C. M. van Hest, *Nat. Commun.* **2020**, *11*, 6282.
[130] M. Moinpour, A. Fracassi, R. J. Brea, M. Salvador-Castell, S. Pandey, M. M. Edwards, S. Seifert, S. Joseph, S. K. Sinha, N. K. Devaraj, *ChemBioChem* **2021**, *23*, 202100624.
[131] D. T. Nguyen, B.-J. Jeon, G. R. Abraham, O. A. Saleh, *Langmuir* **2019**, *35*, 14849.
[132] Q.-H. Zhao, F.-H. Cao, Z.-H. Luo, W. T. S. Huck, N.-N. Deng, *Angew. Chem., Int. Ed.* **2022**, *61*, e202117500.
[133] T. Mashima, M. H. M. E. van Stevendaal, F. R. A. Cornelissens, A. F. Mason, B. J. H. M. Rosier, W. J. Altenburg, K. Oohora, S. Hirayama, T. Hayashi, J. C. M. van Hest, L. Brunsveld, *Angew. Chem., Int. Ed.* **2022**, *61*, e20215041.
[134] N. Martin, M. Li, S. Mann, *Langmuir* **2016**, *32*, 5881.
[135] D. Despotovic, D. S. Tawfik, *ChemSystemsChem* **2021**, *3*, 2100002.
[136] M. Seal, O. Weil-Ktorza, D. Despotovic, D. S. Tawfik, Y. Levy, N. Metanis, L. M. Longo, D. Goldfarb, *J. Am. Chem. Soc.* **2022**, *144*, 20976.
[137] P. M. McCall, S. Srivastava, S. L. Perry, D. R. Kovar, M. L. Gardel, M. V. Tirrell, *Biophys. J.* **2018**, *114*, 1636.
[138] K. A. Ganar, L. Leitjen, S. Deshpande, *ACS Synth. Biol.* **2022**, *11*, 2869.
[139] W. P. Lipinski, B. S. Visser, I. Robu, M. A. A. Fakhree, S. Lindhoud, M. M. A. E. Classens, E. Spruijt, *Sci. Adv.* **2022**, *8*, eabq6495.
[140] S. Alberti, A. A. Hyman, *Nat. Rev. Mol. Cell Biol.* **2021**, *22*, 196.
[141] T. J. Nott, T. D. Craggs, A. J. Baldwin, *Nat. Chem.* **2016**, *8*, 569.
[142] S. Choi, M. O. Meyer, P. C. Bevilacqua, C. D. Keating, *Nat. Chem.* **2022**, *14*, 1110.
[143] T. P. Fraccia, T. Z. Jia, *ACS Nano* **2020**, *14*, 15071.
[144] T. P. Fraccia, N. Martin, *Nat. Commun.* **2023**, *14*, 2606.
[145] T. P. Fraccia, G. Zanchetta, *Curr. Opin. Colloid Interface Sci.* **2021**, *56*, 101500.
[146] A. Jain, S. Kassem, R. S. Fisher, B. Wang, T.-D. Li, T. Wang, Y. He, S. Elbaum-Garfinkle, R. V. Ulijn, *J. Am. Chem. Soc.* **2022**, *144*, 15002.
[147] R. K. Kumar, R. L. Harniman, A. J. Patil, S. Mann, *Chem. Sci.* **2016**, *7*, 5879.
[148] M. Criado-Gonzalez, D. Wagner, M. Haseeb Iqbal, A. Ontani, A. Carvalho, M. Schmutz, J. B. Schlenoff, P. Schaaf, L. Jierry, F. Boulmedais, *J. Colloid Interface Sci.* **2021**, *588*, 580.
[149] S. Zhou, X. Cai, Y. Zhang, Q. Chen, X. Yang, K. Wang, L. Jian, J. Liu, *J. Mater. Chem. B* **2022**, *10*, 8322.
[150] N. Martin, J.-P. Douliez, Y. Qiao, R. Booth, M. Li, S. Mann, *Nat. Commun.* **2018**, *9*, 3652.
[151] M. Zhuang, Y. Zhang, S. Zhou, Y. Zhang, K. Wang, J. Nie, J. Liu, *Chem. Commun.* **2019**, *55*, 13880.
[152] J. Crosby, T. Treadwell, M. Hammerton, K. Vasilakis, M. P. Crump, D. S. Williams, S. Mann, *Chem. Sci.* **2012**, *48*, 11832.
[153] T.-Y. D. Tang, D. van Swaay, A. deMello, J. L. R. Anderson, S. Mann, *Chem. Commun.* **2015**, *51*, 11429.
[154] T. Beneyton, C. Love, M. Girault, T.-Y. D. Tang, J.-C. Baret, *ChemSystemsChem* **2020**, *2*, 2000022.
[155] R. R. Poudyal, R. M. Guth-Metzler, A. J. Veenis, E. A. Frankel, C. D. Keating, P. C. Bevilacqua, *Nat. Commun.* **2019**, *10*, 490.
[156] B. Drobot, J. M. Iglesias-Artola, K. L. Vay, V. Mayr, M. Kar, M. Kreysing, H. Mutschler, T.-Y. D. Tang, *Nat. Commun.* **2018**, *9*, 3643.
[157] R. R. Poudyal, C. D. Keating, P. C. Bevilacqua, *ACS Chem. Biol.* **2019**, *14*, 1243.
[158] J. M. Iglesias-Artola, B. Drobot, M. Kar, A. W. Fritsch, H. Mutschler, T.-Y. D. Tang, M. Kreysing, *Nat. Chem.* **2022**, *14*, 407.

[159] K. L. Vay, E. Y. Song, B. Ghosh, T.-Y. D. Tang, H. Mutschler, *Angew. Chem., Int. Ed.* **2021**, *60*, 26096.
[160] E. Sokolova, E. Spruijt, M. M. K. Hansen, W. T. S. Huck, *Proc. Natl. Acad. Sci. USA* **2013**, *110*, 11692.
[161] W. Stroberg, S. Schnell, *Biophys. J.* **2018**, *115*, 3.
[162] A. Küchler, M. Yoshimoto, S. Luginbühl, F. Mavelli, P. Walde, *Nat. Nanotechnol.* **2016**, *11*, 409.
[163] S. Serrano-Luginbühl, K. Ruiz-Mirazo, R. Ostasewski, F. Gallou, P. Walde, *Nat. Rev. Chem.* **2018**, *2*, 306.
[164] S. Ali, M. Bleuel, V. M. Prabhu, *ACS Macro Lett.* **2019**, *8*, 289.
[165] W. M. Aumiller Jr, F. Pir Cakmak, B. W. Davis, C. D. Keating, *Langmuir* **2016**, *32*, 10042.
[166] H. Kim, B.-j. Jeon, S. Kim, Y. S. Jho, D. S. Hwang, *Polymer* **2019**, *11*, 691.
[167] T. Lu, K. K. Nakashima, E. Spruijt, *J. Phys. Chem. B* **2021**, *125*, 3080.
[168] N. Martin, L. Tian, D. Spencer, A. Coutable-Pennarun, J. L. R. Anderson, S. Mann, *Angew. Chem., Int. Ed.* **2019**, *7*, 14594.
[169] S. Lafon, N. Martin, *Methods Enzymol.* **2021**, *646*, 329.
[170] W. Mu, Z. Ji, M. Zhou, J. Wu, Y. Lin, Y. Qiao, *Sci. Adv.* **2021**, *7*, eabf9000.
[171] Y. Huang, X. Wang, J. Li, Y. Lin, H. Chen, X. Liu, X. Huang, *ChemSystemsChem* **2021**, *3*, 2100006.
[172] W. A. Wee, H. Sugiyama, S. Park, *iScience* **2021**, *24*, 103455.
[173] E. H. Reed, B. S. Schuster, M. C. Good, D. A. Hammer, *ACS Synth. Biol.* **2020**, *9*, 500.
[174] W. M. Aumiller Jr, C. D. Keating, *Nat. Chem.* **2015**, *8*, 129.
[175] K. K. Nakashima, J. F. Baaji, E. Spruijt, *Soft Matter* **2018**, *14*, 361.
[176] K. K. Nakashima, M. H. I. van Haren, A. A. M. André, I. Robu, E. Spruijt, *Nat. Commun.* **2021**, *12*, 3819.
[177] P. R. Banerjee, A. N. Milin, M. M. Moosa, P. L. Onuchic, A. A. Deniz, *Angew. Chem., Int. Ed.* **2017**, *56*, 11354.
[178] S. Deshpande, F. Brandenburg, A. Lau, M. G. F. Last, W. K. Spoelstra, L. Reese, S. Wunnava, M. Dogterom, C. Dekker, *Nat. Commun.* **2019**, *10*, 1800.
[179] W. K. Spoelstra, E. O. van der Sluis, M. Dogterom, L. Reese, *Langmuir* **2020**, *36*, 1956.
[180] J. Deng, A. Walther, *Chem* **2020**, *6*, 3329.
[181] B. S. Schuster, E. H. Reed, R. Parthasarathy, C. N. Jahnke, R. M. Caldwell, J. G. Bermudez, H. Ramage, M. C. Good, D. A. Hammer, *Nat. Commun.* **2018**, *9*, 2985.
[182] M. Matsuo, K. Kurihara, *Nat. Commun.* **2021**, *12*, 5487.
[183] C. Donau, F. Späth, M. Sosson, B. A. K. Kriebisch, F. Schnitter, M. Tena-Solsona, H.-S. Kang, E. Salibi, M. Sattler, H. Mutschler, J. Boekhoven, *Nat. Commun.* **2020**, *11*, 5167.
[184] C. Donau, F. Späth, M. Stasi, A. M. Bergmann, J. Boekhoven, *Angew. Chem., Int. Ed.* **2022**, *61*, e202211905.
[185] D. Zwicker, R. Seyboldt, C. A. Weber, A. A. Hyman, F. Jülicher, *Nat. Phys.* **2017**, *13*, 408.
[186] B. Gouveia, Y. Kim, J. W. Shaevitz, S. Petry, H. A. Stone, C. P. Brangwynne, *Nature* **2022**, *609*, 255.
[187] T. Lu, E. Spruijt, *J. Am. Chem. Soc.* **2020**, *142*, 2905.
[188] G. A. Mountain, C. D. Keating, *Biomacromolecules* **2020**, *21*, 630.
[189] N. G. Moreau, N. Martin, P. Gobbo, T.-Y. D. Tang, S. Mann, *Chem. Commun.* **2020**, *56*, 12717.
[190] R. S. Fisher, S. Elbaum-Garfinkle, *Nat. Commun.* **2020**, *11*, 4628.
[191] Y. Chen, M. Yuan, Y. Zhang, S. Liu, X. Yang, K. Wang, J. Liu, *Chem. Sci.* **2020**, *11*, 8617.
[192] X. Chen, E.-Q. Chen, A.-C. Shi, S. Yang, *ACS Macro Lett.* **2021**, *10*, 1041.
[193] X. Chen, E.-Q. Chen, S. Yang, *Macromolecules* **2023**, *56*, 3.
[194] J. R. Simon, N. J. Carroll, M. Rubinstein, A. Chilkoti, G. P. López, *Nat. Chem.* **2017**, *9*, 509.
[195] T. Kaur, M. Raju, I. Alshareedah, R. B. Davis, D. A. Potoyan, P. R. Banerjee, *Nat. Commun.* **2021**, *12*, 872.
[196] M. Walczak, R. A. Brady, L. Mancini, C. Contini, R. Rubio-Sanchez, W. Y. Kaufhold, P. Cicuta, L. Di Michele, *Nat. Commun.* **2021**, *12*, 4743.
[197] M. Feric, N. Vaidya, T. S. Harmon, D. M. Mitrea, L. Zhu, T. M. Richardson, R. W. Kriwacki, R. V. Pappu, C. P. Brangwynne, *Cell* **2016**, *165*, 1686.
[198] F. Zhorabek, M. S. Abesekara, J. Liu, X. Dai, J. Huang, Y. Chau, *Chem. Sci.* **2023**, *14*, 801.
[199] H. Jing, Q. Bai, Y. Lin, H. Chang, D. Yin, D. Liang, *Langmuir* **2020**, *36*, 8017.
[200] D. R. Scheff, K. L. Weirich, K. Dasbiswas, A. Patel, S. Vaikuntanathan, M. L. Gardel, *Soft Matter* **2020**, *16*, 5659.
[201] A. Hérnandez-Vega, M. Braun, L. Scharrel, M. Jahnel, S. Wegmann, B. T. Hyman, S. Alberti, A. A. Hyman, *Cell Rep.* **2017**, *20*, 2304.
[202] E. te Brinke, J. Groen, A. Hermann, H. A. Heus, G. Rivas, E. Spruijt, W. T. S. Huck, *Nat. Nanotechnol.* **2018**, *13*, 849.
[203] F. Fanalista, S. Deshpande, A. Lau, G. Pawlik, C. Dekker, *Adv. Biosyst.* **2018**, *2*, 1800136.
[204] T. Lu, S. Liese, L. Schoenmakers, C. A. Weber, H. Suzuki, W. T. S. Huck, E. Spruijt, *J. Am. Chem. Soc.* **2022**, *144*, 13451.
[205] A. Mangiarotti, M. Siri, Z. Zhao, L. Malacrida, R. Dimova, *bioRxiv* **2023**, https://doi.org/10.1101/2023.01.04.522768.
[206] A. Mangiarotti, N. Chen, Z. Zhao, R. Lipowsky, R. Dimova, *Nat. Commun.* **2023**, *14*, 2809.
[207] F. Yuan, H. Alimohamadi, B. Bakka, J. C. Stachowiak, *Proc. Natl. Acad. Sci. USA* **2021**, *118*, e2017435118.
[208] H. Kusumaatmaja, A. I. May, M. Feeney, R. L. Knorr, *Proc. Natl. Acad. Sci. USA* **2021**, *118*, e2024109118.
[209] J. Agudo-Canalejo, S. W. Schultz, H. Chino, S. M. Migliano, C. Saito, I. Koyama-Honda, H. Stenmark, A. Brech, A. I. May, N. Mizushima, R. L. Knorr, *Nature* **2021**, *591*, 142.
[210] M. Weiss, J. P. Frohnmayer, L. T. Benk, B. Haller, J.-W. Janiesch, T. Heitkamp, M. Börsch, R. B. Lira, R. Dimova, R. Lipowsky, E. Bodenschatz, J.-C. Baret, T. Vidakovic-Koch, K. Sundmacher, I. Platzman, J. P. Spatz, *Nat. Mater.* **2018**, *17*, 89.
[211] M. Linsenmeier, M. R. G. Kopp, S. Stavrakis, A. de Mello, P. Arosio, *Biochim. Biophys. Acta, Mol. Cell Res.* **2021**, *1868*, 118823.
[212] A. M. Bergmann, C. Donau, F. Späth, K. Jahnke, K. Göpfrich, J. Boekhoven, *Angew. Chem., Int. Ed.* **2022**, *61*, e202203928.
[213] M. Linsenmeier, M. R. G. Kopp, F. Grigolato, L. Emmanoulidis, D. Liu, D. Zürcher, M. Hondele, K. Weis, U. Capasso Palmiero, P. Arosio, *Angew. Chem., Int. Ed.* **2019**, *58*, 14489.
[214] W. E. Arter, R. Qi, N. A. Erkamp, G. Krainer, K. Didi, T. J. Welsh, J. Acker, J. Nixon-Abell, S. Qamar, J. Guillén-Boixet, T. M. Franzmann, D. Kuster, A. A. Hyman, A. Borodavka, P. S. George-Hyslop, S. Alberti, T. P. J. Knowles, *Nat. Commun.* **2022**, *13*, 7845.
[215] N.-N. Deng, W. T. S. Huck, *Angew. Chem., Int. Ed.* **2017**, *56*, 9736.
[216] R. Booth, Y. Qiao, M. Li, S. Mann, *Angew. Chem., Int. Ed.* **2019**, *58*, 9120.
[217] C. Love, J. Steinkühler, D. T. Gonzales, N. Yandrapalli, T. Robinson, R. Dimova, T.-Y. D. Tang, *Angew. Chem., Int. Ed.* **2020**, *59*, 5950.
[218] M. G. F. Last, S. Deshpande, C. Dekker, *ACS Nano* **2020**, *14*, 4487.
[219] H. Seo, H. Lee, *Nat. Commun.* **2022**, *13*, 5179.
[220] J. Li, M. Zhu, S. Wang, Z. Tao, X. Liu, X. Huang, *Chem. Commun.* **2021**, *57*, 11713.
[221] H. Zhao, V. Ibrahimova, E. Garanger, S. Lecommandoux, *Angew. Chem., Int. Ed.* **2020**, *59*, 11028.
[222] H. Zhao, E. Ibarboure, V. Ibrahimova, Y. Xiao, E. Garanger, S. Lecommandoux, *Adv. Sci.* **2021**, *8*, 2102508.
[223] C. Schvartzman, H. Zhao, E. Ibarboure, V. Ibrahimova, E. Garanger, S. Lecommandoux, *Adv. Mater.* **2023**, 2301856.
[224] H. Li, Y. Yan, J. Chen, K. Shi, C. Song, Y. Ji, L. Jia, J. Li, Y. Qiao, Y. Lin, *Sci. Adv.* **2023**, *9*, eade5853.

[225] S. Song, A. Llopis-Lorente, A. F. Mason, L. K. E. Abdelmoshen, J. C. M. van Hest, *J. Am. Chem. Soc.* **2022**, *144*, 13831.
[226] M. Chen, G. Liu, M. Zhang, Y. Li, X. Hong, H. Yang, *Small* **2023**, *19*, 2206437.
[227] L. Tian, M. Li, J. Liu, A. J. Patil, B. W. Drinkwater, S. Mann, *ACS Cent. Sci.* **2018**, *4*, 1551.
[228] X. Wang, L. Tian, Y. Ren, Z. Zhao, H. Du, Z. Zhang, B. W. Drinkwater, S. Mann, X. Han, *Small* **2020**, *16*, 1906394.
[229] P. Zhan, K. Jahnke, N. Liu, K. Göpfrich, *Nat. Chem.* **2022**, *14*, 958.
[230] M. P. Tran, R. Chatterjee, Y. Dreher, J. Fichtler, K. Jahnke, L. Hilbert, V. Zaburdaev, K. Göpfrich, *Small* **2023**, *19*, 2202711.
[231] K. A. Ganar, L. W. Honaker, S. Deshpande, *Curr. Opin. Colloid Interface Sci.* **2021**, *54*, 101459.
[232] D. van Swaay, T.-Y. D. Tang, S. Mann, A. de Mello, *Angew. Chem., Int. Ed.* **2015**, *54*, 8398.
[233] A. Agrawal, J. F. Douglas, M. Tirrell, A. Karim, *Proc. Natl. Acad. Sci. USA* **2022**, *119*, e2203483119.
[234] N. Gao, S. Mann, *Acc. Chem. Res.* **2023**, *56*, 297.
[235] F. Pir Cakmak, A. T. Grigas, C. D. Keating, *Langmuir* **2019**, *35*, 7830.
[236] Q. Li, Q. Song, W. Guo, Y. Cao, Y. Chao, X. Cui, J. Wei, D. Chen, H. C. Shum, *bioRxiv* **2022**, https://doi.org/10.1101/2021.02.19.432011.
[237] J. Fothergill, M. Li, S. A. Davis, J. A. Cunningham, S. Mann, *Langmuir* **2014**, *30*, 14591.
[238] N. Gao, C. Xu, Z. Yin, M. Li, S. Mann, *J. Am. Chem. Soc.* **2022**, *144*, 3855.
[239] A. Jobdeedamrong, S. Cao, I. Harley, D. Crespy, K. Landfester, L. Caire da Silva, *Nanoscale* **2023**, *15*, 2561.
[240] R. Toor, A. Neujahr Copstein, C. Trébuchet, B. Goudeau, P. Garrigue, V. Lapeyre, A. Perro, V. Ravaine, *J. Colloid Interface Sci.* **2023**, *630*, 66.
[241] C. Zhao, J. Li, S. Wang, Z. Xu, X. Wang, X. Liu, L. Wang, X. Huang, *ACS Nano* **2021**, *15*, 10048.
[242] S. Liu, Y. Zhang, M. Li, L. Xiong, Z. Zhang, X. Yang, X. He, K. Wang, J. Liu, S. Mann, *Nat. Chem.* **2020**, *12*, 1165.
[243] C. Xu, N. Martin, M. Li, S. Mann, *Nature* **2022**, *609*, 1029.
[244] T.-Y. D. Tang, C. R. Che Hak, A. J. Thomson, M. K. Kuimova, D. S. Williams, A. W. Perriman, S. Mann, *Nat. Chem.* **2014**, *6*, 527.
[245] H. Jing, Y. Lin, H. Chang, Q. Bai, D. Liang, *Langmuir* **2019**, *35*, 5587.
[246] F. Pir Cakmak, A. M. Marianelli, C. D. Keating, *Langmuir* **2021**, *37*, 10366.
[247] Y. Zhang, Y. Chen, X. Yang, X. He, M. Li, S. Liu, K. Wang, J. Liu, S. Mann, *J. Am. Chem. Soc.* **2021**, *143*, 2866.
[248] J. Son, Y. Jung, *Chem. Sci.* **2022**, *13*, 11841.
[249] S. Liu, Y. Zhang, X. He, M. Li, J. Huang, X. Yang, K. Wang, S. Mann, J. Liu, *Nat. Commun.* **2022**, *13*, 5254.
[250] C.-W. Yeh, Y. Wang, *Macromol. Biosci.* **2023**, *23*, 2200538.
[251] H. Chang, H. Jing, Y. Yin, Q. Zhang, D. Liang, *Chem. Commun.* **2018**, *54*, 13849.
[252] C. Yin, Z. Lin, X. Jiang, N. Martin, L. Tian, *ACS Appl. Mater. Interfaces* **2023**, *15*, 27447.
[253] J. Li, X. Liu, L. K. E. A. Abdelmohsen, D. S. Williams, X. Huang, *Small* **2019**, *15*, 1902893.
[254] S. Gao, S. Srivastava, *ACS Macro Lett.* **2022**, *11*, 902.
[255] A. F. Mason, B. C. Buddingh', D. S. Williams, J. C. M. van Hest, *J. Am. Chem. Soc.* **2017**, *139*, 17309.
[256] A. F. Mason, N. A. Yewdall, P. L. W. Welzen, J. Shao, M. van Stevendaal, J. C. M. van Hest, D. S. Williams, L. K. E. A. Abdelmohsen, *ACS Cent. Sci.* **2019**, *5*, 1360.
[257] N. A. Yewdall, B. C. Buddingh, W. J. Altenburg, S. B. P. E. Timmermans, D. F. M. Vervoort, L. K. E. A. Abdelmohsen, A. F. Mason, J. C. M. van Hest, *ChemBioChem* **2019**, *20*, 2643.
[258] M. H. M. E. van Stevendaal, L. Vasiukas, N. A. Yewdall, A. F. Mason, J. C. M. van Hest, *ACS Appl. Mater. Interfaces* **2021**, *13*, 7879.
[259] J.-P. Douliez, N. Martin, T. Beneyton, J.-C. Eloi, J.-P. Chapel, L. Navailles, J.-C. Baret, S. Mann, L. Béven, *Angew. Chem., Int. Ed.* **2018**, *57*, 7780.
[260] K. D. Seo, S. Shin, H. Y. Yoo, J. Cao, S. Lee, J.-W. Yoo, D. S. Kim, D. S. Hwang, *Biomacromolecules* **2020**, *21*, 930.
[261] R. Toor, L. Hourdin, S. Shanmugathasan, P. Lefrançois, S. Arbault, V. Lapeyre, L. Bouffier, J.-P. Douliez, V. Ravaine, A. Perro, *J. Colloid Interface Sci.* **2023**, *629*, 46.
[262] E. Magdalena Estirado, A. F. Mason, M. A. Alemán García, J. C. M. van Hest, L. Brunsveld, *J. Am. Chem. Soc.* **2020**, *142*, 9106.
[263] N. Coudon, L. Navailles, F. Nallet, I. Ly, A. Bentaleb, J.-P. Chapel, L. Béven, J.-P. Douliez, N. Martin, *J. Colloid Interface Sci.* **2022**, *617*, 257.
[264] S. Song, A. F. Mason, R. A. J. Post, M. De Corato, R. Mestre, N. A. Yewdall, S. Cao, R. W. van der Hofstad, S. Sanchez, L. K. E. A. Abdelmohsen, J. C. M. van Hest, *Nat. Commun.* **2021**, *12*, 6897.
[265] B. V. V. S. P. Kumar, J. Fothergill, J. Bretherton, L. Tian, A. J. Patil, S. A. Davis, S. Mann, *Chem. Commun.* **2018**, *54*, 3594.
[266] J. B. Woodruff, B. F. Gomes, P. O. Widlund, J. Mahamid, A. Honigmann, A. A. Hyman, *Cell* **2017**, *169*, 1066.
[267] X. Wang, S. Wu, T.-Y. D. Tang, L. Tian, *Trends Chem.* **2022**, *4*, 1106.

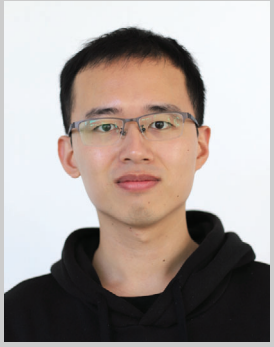

Zi Lin received his B.E. and M.E. degrees in biomedical engineering from the Sun Yat-Sen University in 2017 and 2020, respectively. After studying as a research assistant in the Zhejiang University in 2020–2021, he is currently pursuing his Ph.D. degree in physical chemistry of condensed matter at the University of Bordeaux, France, in the Centre de Recherche Paul Pascal, under the supervision of Prof. Jean-Christophe Baret and Dr. Nicolas Martin. His research focuses on the dynamic behavior of light-responsive coacervate droplets.

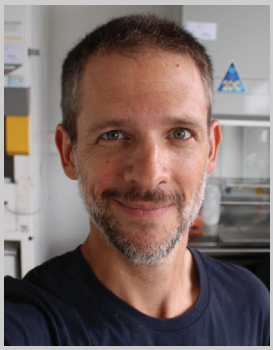

Thomas Beneyton is a CNRS Research Engineer at the Centre de Recherche Paul Pascal (CRPP) in Pessac, France. He obtained is Ph.D. at the University of Strasbourg, focusing on droplet-based microfluidics for the directed evolution of proteins. Later, he moved to the ESPCI Laboratory of BioChemistry in Paris as a postdoc to use microfluidic technology for the functional screening of microbial populations. He then joined the CRPP as a MaxSynBio Fellow to work on the microfluidic assembly of functional artificial cells. Currently, his work focuses on microfluidic technology either for single-cell screening or bottom-up synthetic biology applications.

Jean-Christophe Baret is professor at the University of Bordeaux and Group Leader at the Centre de Recherche Paul Pascal, a joint research lab from the CNRS and the University of Bordeaux. He applies his soft matter physics and microfluidics expertise to biological systems, to design methodologies for high-throughput screening and more recently for the assembly of synthetic cells.

Nicolas Martin is CNRS Researcher at the Centre de Recherche Paul Pascal, University of Bordeaux, France. After completing his Ph.D. at the Ecole Normale Supérieure in Paris on polyelectrolyte-assisted protein folding, he expanded his research on synthetic cells in the group of Prof. Stephen Mann FRS at the University of Bristol, UK. His current research interests focus on the design and characterization of stimuli-responsive complex coacervates based on polyelectrolytes, nucleic acids, peptides, or amphiphiles to mimic the dynamic intracellular organization and shed light on the emergence of self-assembled life-like compartments.